Marine Pollution Bulletin 126 (2018) 501–515

Contents lists available at ScienceDirect

Marine Pollution Bulletin

journal homepage: www.elsevier.com/locate/marpolbul

Experimental leaching of massive sulphide from TAG active hydrothermal mound and implications for seafloor mining

Emily K. Fallon[a,b,*], Ella Niehorster[a], Richard A. Brooker[b], Thomas B. Scott[a]

[a] Interface Analysis Centre, School of Physics, HH Wills Physics Laboratory, University of Bristol, Tyndall Ave., BS8 1TL, UK
[b] School of Earth Sciences, University of Bristol, Wills Memorial Building, Queens Rd, BS8 1RJ, UK

ARTICLE INFO

Keywords:
SMS deposits
Mining impact
Leaching
Metal release
Toxicity

ABSTRACT

Seafloor massive sulphide samples from the Trans-Atlantic Geotraverse active mound on the Mid-Atlantic Ridge were characterised and subjected to leaching experiments to emulate proposed mining processes. Over time, leached Fe is removed from solution by the precipitation of Fe oxy-hydroxides, whereas Cu and Pb leached remained in solution at ppb levels. Results suggest that bulk chemistry is not the main control on leachate concentrations; instead mineralogy and/or galvanic couples between minerals are the driving forces behind the type and concentration of metals that remain in solution. Dissolved concentrations exceed ANZECC toxicity guidelines by 620 times, implying the formation of localised toxicity in a stagnant water column. Moreover, concentrations will be higher when scaled to higher rock-fluid ratios and finer grain sizes proposed for mining scenarios. The distance at which dilution is achieved to meet guidelines is unlikely to be sufficient, indicating a need for the refinement of the mining process.

1. Introduction

As the global demand for metals continues to grow, driven by advances in technology, so does the market price. With the majority of economically viable terrestrial resources already exploited and fewer being discovered, previously disregarded sources of metals are now beginning to be more seriously considered. Heightened interest in seafloor exploration is highlighted by governments and commercial enterprises already applying for and receiving licenses for exploration, with 27 exploration licenses issued by the International Seabed Authority (ISA) as of 2017, covering upwards of 1.2 million - square kilometres of the seafloor (ISA, 2017). Additionally, whilst more difficult to track, there are an estimated 26 exploration projects within national jurisdiction areas of individual states' economic exclusion zones (EEZs) (ECORYS, 2014). Further to this, 78 submissions have been made by 68 different territories to extend their continental shelf and subsequently their economic exclusion zone to lay claim to larger expanses of the seafloor and associated mineral resources (CLCS, 2017). Advances in deep-sea oil and gas extraction technology have paved the way for the economic viability of deep-sea mining. As a result, expectations are high that this industry is about to emerge.

Seafloor massive sulphide (SMS) ore deposits and their economic worth has been discussed extensively in the literature (German et al., 2016; Hannington and Jamieson, 2011; Hannington et al., 2010; Monecke et al., 2016), with Nautilus Minerals Inc. already in the process of planning mineral extraction in what would be the world's first SMS mine at the Solwara 1 deposit in the Bismarck Sea off Papua New Guinea. In order to support any future economic potential, our knowledge and understanding of such deposits requires significant improvement with an associated need for assessment of any environmental impact that any future endeavours may produce.

Sulphide minerals at both active and inactive hydrothermal seafloor vents undergo chemical interaction with seawater. This generally results in oxidative weathering (Edwards, 2004a), a process similar to the weathering that occurs in their terrestrial counterparts – volcanogenic massive sulphide (VMS) deposits. On land in restricted drainage systems, this occurs more vigorously at decreasing values of pH and can result in acid mine drainage (AMD), which promotes further dissolution as shown for pyrite in Eqs. (1) & (2).

$$FeS_2 + 3.5O_2\,(aq) + H_2O \rightarrow Fe^{2+} + 2SO_4^{2-} + 2H^+ \quad (1)$$

$$FeS_2 + 14Fe^{3+} + 8H_2O \longrightarrow 15Fe^{2+} + 2SO_4^{2-} + 16H^+ \quad (2)$$

In contrast, this equivalent weathering process on the seafloor occurs in waters of near neutral pH and of almost 'infinite' volume, so that arising acidity from oxidation is almost immediately buffered and low pH conditions will not develop over a significant area due to the dilution effect. The reactions result in formation of insoluble oxy-hydroxide

* Corresponding author at: Interface Analysis Centre, School of Physics, HH Wills Physics Laboratory, University of Bristol, Tyndall Ave., BS8 1TL, UK.
E-mail address: e.fallon@bristol.ac.uk (E.K. Fallon).

https://doi.org/10.1016/j.marpolbul.2017.10.079
Received 24 April 2017; Received in revised form 1 September 2017; Accepted 27 October 2017

minerals such as goethite and hematite at the expense of sulphides such as pyrite, as illustrated in Eqs. (3) & (4) (Mills and Elderfield, 1995; Edwards, 2004b). These Fe oxide minerals can accumulate as crusts or caps on sulphide deposits on the seafloor and are referred to as 'gossans' with the mineral mixtures often referred to as limonite (Herzig and Hannington, 1995).

$$2FeS_2 + 7.5O_2\,(aq) + 4H_2O \rightarrow Fe_2O_3 + 4SO_4^{2-} + 8H^+ \quad (3)$$

$$FeS_2 + 3.75O_2(aq) + 3.5H_2O \rightarrow Fe(OH)_3 + 2SO_4^{2-} + 4H^+ \quad (4)$$

In terms of Cu, Zn and Pb bearing sulphide minerals and the fate of these other metals throughout the natural oxidation process, the mineral products formed vary, including atacamite (copper chloride hydroxide that can also host Zn and Pb), sulphates (Pb - anglesite), hydrous sulphates (Pb – plumbojarosite, Zn - goslarite), carbonates (Zn - smithsonite, Pb - cerussite) as well as native copper. However, the processes and pH conditions at which these minerals form also vary, where reduced dissolved species of these metals are much more soluble than Fe, explaining the dominance of Fe oxides and oxy-hydroxides in seafloor gossans (Koski, 2012; Ridley, 2012). Metal sulphates generally form at lower pH (< 6) conditions with reduced seawater circulation, seawater-stable atacamites form where acidic pore waters carrying dissolved Cu meet surrounding seawater (pH 6–8) and carbonates form later at higher pH, oxidised seawater conditions (Hannington, 1993; Koski, 2012; Mann and Deutscher, 1980; Patwardhan, 2012; Taylor, 2011). Whilst Zn and Pb sulphates have been observed in gossans associated with VMS deposits, there is limited observation of them in SMS gossans (in particular Zn sulphate), expected to be a result of their more acidic formation conditions and high solubility when compared to carbonates (Koski, 2012; Patwardhan, 2012; Ridley, 2012; Seal and Foley, 2002). In addition to the formation of weathering products, Fe oxides and oxy-hydroxides are known to have a high adsorptive capacity, creating a sink for metals such as Cu, Zn and Pb as well as others including Co and As (Balistrieri and Murray, 1982; Benjamin and Leckie, 1981; Jong and Parry, 2004; Liu and Huang, 2003; Ridley, 2012; Rose and Bianchi-Mosquera, 1993). Adsorption of trace metals onto (and subsequently into) iron oxides and oxy-hydroxides is observed to be rapid, on the time scale of hours (Ahmad et al., 2012; Balistrieri and Murray, 1982) so it likely to be an important process on the timescale of this study as well as the actual mining operation.

The process of deep-sea mining has the potential to expose a high surface area of fresh sulphide minerals to the corrosive effects of seawater, allowing for an anthropogenic leaching of metals that is more akin to acid mine drainage observed in a terrestrial setting (Gwyther, 2008; Parry, 2008; Simpson et al., 2007). The only current concept for SMS mining is provided by Nautilus Minerals Inc. and includes an 'in situ' extraction phase that produces 80% < 25 mm and 20% smaller unknown particle size material (where 30% of cut material is initially lost and up to 10% will remain on the seafloor). This is combined with a dewatering process that occurs as the mineral slurry (1:9 rock to fluid ratio) is carried to the surface, isolated via a pipe where it is only in contact with bottom seawater mixed in during 'in situ' extraction, processed above sea level, and the waste water is returned to 25 to 50 m above the seafloor containing < 8 μm sulphide particles at 6.35 g/L rock to fluid ratio (Gwyther, 2008). Both 'in situ' extraction and discharge of return water involve the entrainment of fresh sulphide material into an advective environment, with the dewatering process also providing exposure of sulphide to warmer temperature at the sea surface (Gwyther, 2008).

If any leaching of metals is not balanced by precipitation of oxides, there is the potential for local accumulation of dissolved heavy metals in the water column. These metals may bioaccumulate in local ecosystems, disperse or accumulate in the wider ocean or ultimately precipitate elsewhere as oxides. Mining of SMS deposits and exposure of significant fresh surface area thus has the potential to exaggerate the natural weathering process (Fallon et al., 2017).

The majority of previous dissolution studies to examine metal leaching are related to terrestrial acid mine drainage arising from mine flooding and leaching of tailings piles by meteoric waters (Acero et al., 2009; Bonnissel-Gissinger et al., 1998; Constantin and Chiriţă, 2013; Descostes et al., 2004; Kwong et al., 2003; McKibben and Barnes, 1986; Moses et al., 1987). A small number of dissolution studies of specific sulphide minerals in seawater have been undertaken (Bilenker, 2011; Bilenker et al., 2016; Feely et al., 1987; Romano, 2012) and demonstrate the large difference in oxidation rates between different sulphide minerals, in particular, the two order of a magnitude difference in abiotic oxidation rates between pyrrhotite and chalcopyrite. These rates quantitatively predict that any acid production from 'in situ' mining of SMS deposits will be buffered by advecting seawater and that mine waste has the potential to persist on the seafloor for years without complete oxidative transformation (Bilenker et al., 2016). However, these studies are typically undertaken with relatively large grain size fractions > 45 μm and are representative of 'in situ' mining/extraction rather than the potentially more impactful dewatering and return processes that involves grains < 8 μm. Furthermore, these studies do not take into consideration any potential galvanic effects that may occur within a natural SMS ore that contains a range of co-existing sulphide minerals. A galvanic cell occurs where two different sulphide minerals are touching in the presence of an electrolyte such as seawater. The mineral with the lower resting potential behaves as an anode and preferentially dissolves, protecting the other mineral which is behaving as a cathode (Fig. 1; Mehta and Murr, 1983). As highlighted by Heidel et al. (2013), pyrite in contact with most common SMS sulphide minerals should be galvanically protected as a result of a high rest potential compared to the other most common sulphides (Fig. 1). Within a seafloor context (higher pHs), this is similarly expected to be the case; where even though rest potentials are lower, the relative difference of rest potential between the minerals is constant. Galvanic cells have already been shown to increase dissolution and explain observations within the context of terrestrial sulphide ore deposits (Abraitis et al., 2004a; Heidel et al., 2013; Koski et al., 2008; Kwong et al., 2003; Li et al., 2006; Liu et al., 2008) and have also been put forward to explain observations of the mineralogy of oxidised SMS deposits (Webber et al., 2015). Whilst not attributed to galvanic cells Edwards et al. (2003) demonstrated that a mixed sulphide ore is notably more reactive on the seafloor than individual sulphide minerals, albeit in the presence of bacteria.

SMS deposits are comprised of a variety of mineral grains, each often containing various inclusions, and it is the galvanic interaction of these phases that may have the ability to substantially increase dissolution rates. The only leaching study that simulates natural mixed sulphide rich sediments in seawater was undertaken as a result of prospecting and a regulatory need to provide an environmental impact statement (EIS) for mining the Solwara-1 Deposit, Bismark Sea, Papua New Guinea (Gwyther, 2008). There are two parts to that study, the first undertaken by Australia's Commonwealth Scientific and Industrial Research Organisation (CSIRO) (Simpson et al., 2007), the second undertaken by Charles Darwin University (Parry, 2008). Whilst extensive leaching of a range of metals is observed, the mineralogy of the ore used in experiments is not documented and only the bulk chemistry of the ores is available (as reported in Supplementary material A).

There is clearly a need for further studies that attempt to reproduce the true compositional range of the materials that will be dispersed into the water column as a result of deep sea mining in a colder, deeper (high pressure) more saline, and alkaline aqueous medium. This suspended particulate will include a variety of minerals, many or which will have interfaces (or inclusions) that could lead to galvanic cells. These have the ability to substantially increase the leaching of metals into the water column (Abraitis et al., 2004b; Heidel et al., 2013; Koleini et al., 2010; Kwong et al., 2003; Li et al., 2006; Liu et al., 2008; Majuste et al., 2012; Mehta and Murr, 1983; Subrahmanyam and Forssberg, 1993). There are a multitude of variables to consider in this

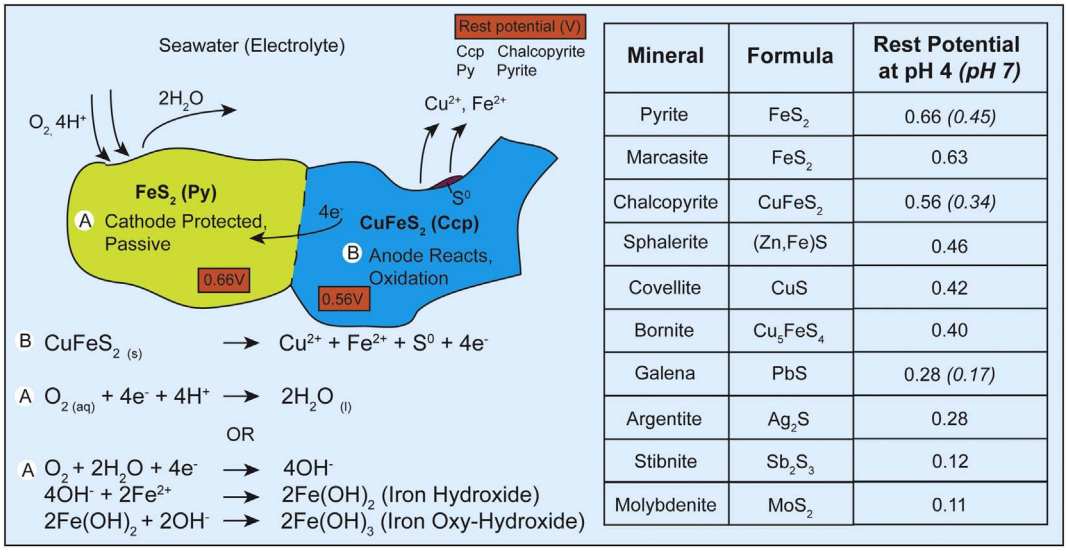

Mineral	Formula	Rest Potential at pH 4 *(pH 7)*
Pyrite	FeS_2	0.66 *(0.45)*
Marcasite	FeS_2	0.63
Chalcopyrite	$CuFeS_2$	0.56 *(0.34)*
Sphalerite	(Zn,Fe)S	0.46
Covellite	CuS	0.42
Bornite	Cu_5FeS_4	0.40
Galena	PbS	0.28 *(0.17)*
Argentite	Ag_2S	0.28
Stibnite	Sb_2S_3	0.12
Molybdenite	MoS_2	0.11

Fig. 1. A galvanic cell occurs when two sulphide minerals with different rest potentials are coupled together in a solution that acts as an electrolyte (seawater in this case). The mineral with the higher rest potential behaves as a cathode (e.g. pyrite) and is galvanically protected with the reduction reaction occurring on its surface. The mineral with the lower rest potential (e.g. chalcopyrite) behaves as an anode and is preferentially dissolved with oxidative dissolution occurring on its surface. There are a number of potential reduction reactions that occur on the surface of the cathode depending on the ions available; shown above are the formation of water as well as hydroxides that can then ultimately form Fe hydroxides/oxy-hydroxides if ferrous Fe is available.
Figure adapted from Murr (2006) and Fallon et al. (2017). Rest potentials of minerals at pH 4 are taken from Majima (1969) and references therein; quoted where available are rest potentials of minerals at pH 7 in distilled water, taken from Cheng and Iwasaki (1992).

process including mineralogy, bulk elemental chemistry, grain size distribution and surface area of the particles, pH, temperature, pressure, salinity, dissolved oxygen and prevailing ocean currents. Mineralogy and geochemistry varies considerably across sulphide ore deposits (Cherkashev et al., 2013; Hannington et al., 2005) as a result of factors including tectonic setting (influencing the composition of the host rock), pressure, pH and temperature. As a result of this, different extant ore deposits are expected to be oxidising and releasing a variety of different metals into the oceans, all at different rates.

In this study, we begin to evaluate the potential for anthropogenic leaching of SMS material as a result of future seafloor mining. The important questions are: Whether leaching occurs and to what extent; Are certain deposits more of an environmental risk to mine and require greater dilutions to meet toxicity guidelines; How will mineralogy and geochemistry play a role in this process. To address some of these questions we have performed a series of leaching experiments that investigate some of these variables for the TAG active mound. In particular, the selected samples represent the diverse mineralogy from within this single SMS deposit.

Three terms are used within this study to refer to the different processes occurring during leaching. **Leaching** is the total loss of mineral solutes by the action of a liquid (seawater). In this context, the loss of minerals (sulphides) is a result of their oxidative dissolution in seawater. The total amount of metals leached (lost) is not necessarily **dissolved** in the subsequent leachate (seawater) due to the **precipitation** of Fe oxide/oxy-hydroxides and sequestration of metals onto oxides. The term **dissolved** refers to the metals remaining in the seawater (after filtration and removal of oxides).

2. Materials

Samples from the TAG active hydrothermal mound Mid-Atlantic Ridge (MAR) were supplied through the Ocean Drilling Program (ODP). Cores were recovered from five sites across the TAG hydrothermal mound (Fig. 2) during Leg 158 of the ODP between October and November 1994 (Humphris et al., 1995, 1996). The five areas are named TAG-1 to TAG-5, where TAG-1 is located closest to the centre of the mound, approximately 20 m SE of the black smoker complex. 3 TAG samples were chosen for experiments as a result of their range in mineralogy as well as availability of material. TAG samples H and J are taken from TAG-4 area, west of the central black smoker complex and TAG B is taken from TAG-3, SW of the Kremlin area (Fig. 2).

An aliquot of each TAG sample was cut, mounted in epoxy and polished as a block for characterisation of the whole rock sample. The remainder was crushed using a pestle and mortar and dry sieved to a size of < 45 μm.

To ensure that any observed heavy metal leaching is a true reflection of the surface area with clean surface (as though freshly mined) and to control grain size, all fine sulphide and oxide particles (< 2.5 μm) were removed.

Whilst there is the potential for a range of distributions within this size fraction (2.5–45 μm), this potential should be eliminated during the normalisation of the data to the surface area of each specific sample (discussed in 3.2). As a result of mixed sulphides being used in experiments and the high solubility of sphalerite and galena at low pH (Abraitis et al., 2004b; Heidel et al., 2013; Malmström and Collin, 2004; Weisener et al., 2004), a cleaning method was adapted from Romano (2012). The cleaning method included 5 min of ultrasonication in acetone, a 5 min ethanol rinse through 2.5 μm filter paper, drying in a desiccator, agitation in 1 M HCl for 30 s followed by a 5 min soak, with a final ethanol rinse through 2.5 μm filter paper before drying in a vacuum desiccator.

This cleaned 2.5–45 μm size fraction was always stored at room temperature in a vacuum desiccator to prevent oxidation, and individual aliquots were removed for characterisation and leaching experiments.

3. Characterisation

TAG samples were characterised as polished blocks as well as cleaned powders prior to leaching experiments. Unfortunately, it should be noted that reacted sulphide material (and any oxide phases that had formed during the experiment) was not retrieved or analysed posterior to experiments.

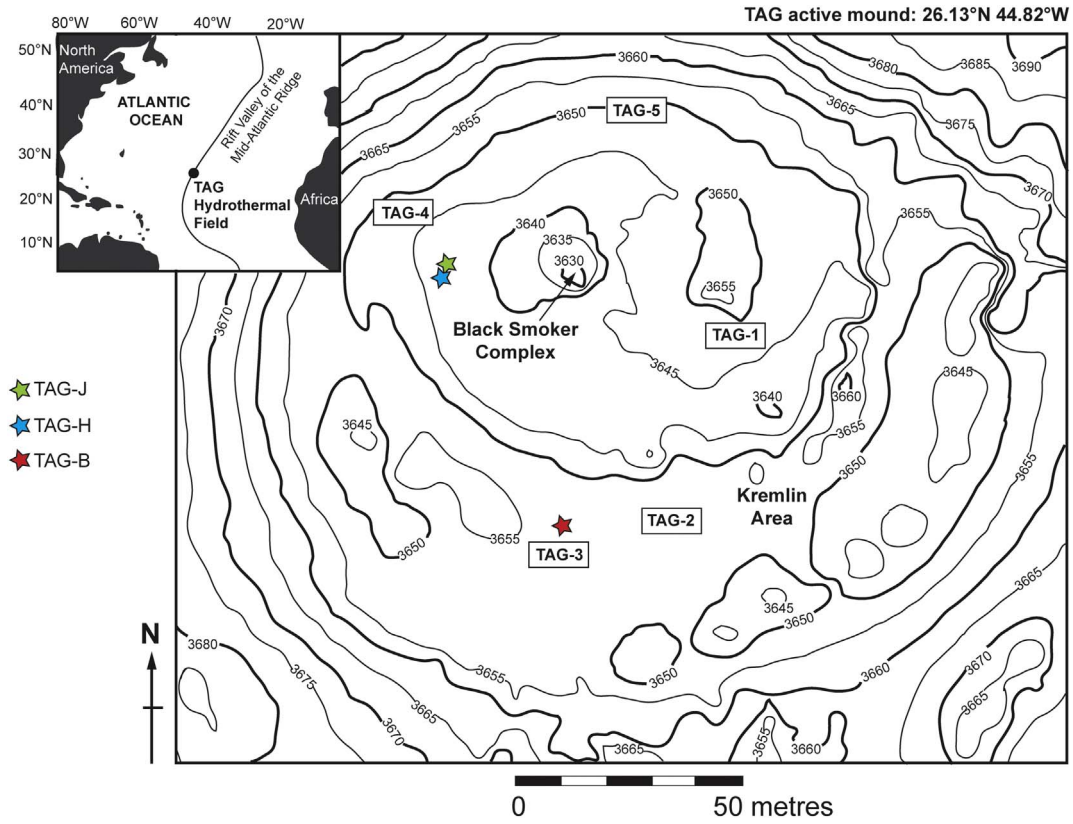

Fig. 2. The location of TAG samples used in this study. TAG-B is located in the TAG-3 area and TAG-H and J in the TAG-4 area. Detailed bathymetric data are overlaid on the map and the inset shows the location of the TAG hydrothermal field within the context of the Atlantic Ocean.
This figure is reproduced from Humphris et al. (1995).

3.1. Sulphide blocks

Polished blocks of each sample were examined by reflected light microscopy to identify the major ore minerals and subsequent scanning electron microscopy (SEM) with an energy-dispersive X-ray (EDX) detector for further identification of phases and their semi-quantitative elemental compositions. The SEM instrument used was a Carl Zeiss Sigma™ variable pressure SEM with a Gemini™ field emission electron column with Octane-Plus™ silicon drift detector. The instrument utilises TEAM analytical software from EDAX. Table 1 provides a summary of the phases identified, their abundances (wt%), textures and the inclusions observed. Representative reflected light photographs of each sample along with SEM backscattered images are shown in Fig. 3.

In addition, some laser ablation-inductively coupled plasma-mass spectrometry (LA-ICP-MS) spot analysis (wt% ppm) were collected on some Cu-poor phases (included in Table 2). These data were collected to help provide an explanation of dissolution results as well as an indication of which minerals are likely to be dissolving. LA-ICP-MS analyses were carried out using a Nu Instruments ATTOM HR-ICP-MS at GEOMAR, Helmholtz Centre for Ocean Research, Kiel. For detailed methodology, please refer to Supplementary material B.

3.2. Sulphide powder

Powder XRD was conducted using a Phillips X'Pert Pro diffractometer with a Cu Kα source; detailed methodology is outlined in Supplementary material C. This provided an overall representation of the phases present including semi-quantitative analysis presented in Table 1 with individual XRD patterns shown in Supplementary material C1. An aliquot of each cleaned sulphide powder was mounted in resin and polished to 1 μm diamond grade. This allowed for identification of mineralogy of individual grains and inclusions (Fig. 4). Bulk Fe and Cu data of all powder samples are also presented in Table 1. Samples underwent aqua regia digestion, with arising solutions analysed on an SPECTRO Ciros SOP inductively coupled plasma - optical emission spectrometer (ICP-OES) at the University of Kiel, Germany. For a more detailed methodology, please refer to Supplementary material D.

Surface area analysis was undertaken to highlight any differences

Table 1
Sample list with quoted surface area from BET measurements of ground, sieved and cleaned massive sulphide powders (2.5–45 μm). Semi quantitative data (wt%) are presented based on powder X-ray diffraction of ground, sieved and cleaned sulphide powders (2.5–45 μm), dashes indicate either no observation or that the concentration was below the detection limit. Also presented are observations of inclusions based upon reflected light microscopy and SEM, EDX. Abbreviations used here are *Py* (pyrite), *Mc* (marcasite), *Ccp* (chalcopyrite), *Cv* (covellite), *Sp* (sphalerite), *Anh* (anhydrite), *Ox* (Fe oxides/oxy-hydroxides) and qtz (quartz). Bulk Fe, Cu and Pb concentration determined by aqua regia digestion with ICP-OES. Detailed method of acid digestion included in Supplementary material D.

Location	Sample	Surface area	Mineral abundances (wt%)									Inclusions	Bulk Fe	SD	Bulk Cu	SD	Bulk Pb	SD
		(m^2/g)	Py	Mc	Ccp	Cv	Sp	Anh	Ox	Atc	Qtz		wt%		ppm		ppm	
TAG-3	TAG-B	1.843	19.7	2.5	5.2	–	–	–	19.5	3.9	49.1	ccp in py, py in ccp	25.8	1.0	43,035	5	183	7
TAG-4	TAG-H	0.552	38.4	44.3	–	–	1.2	0.8	1.7	–	10.7	sp in py, mc	44.4	3.8	1130	86	108	9
TAG-4	TAG-J	0.607	84.2	5.8	4.7	1.4	0.7	0.5	–	–	2.7	sp, ccp in py	45.3	5.3	36,592	4073	164	19

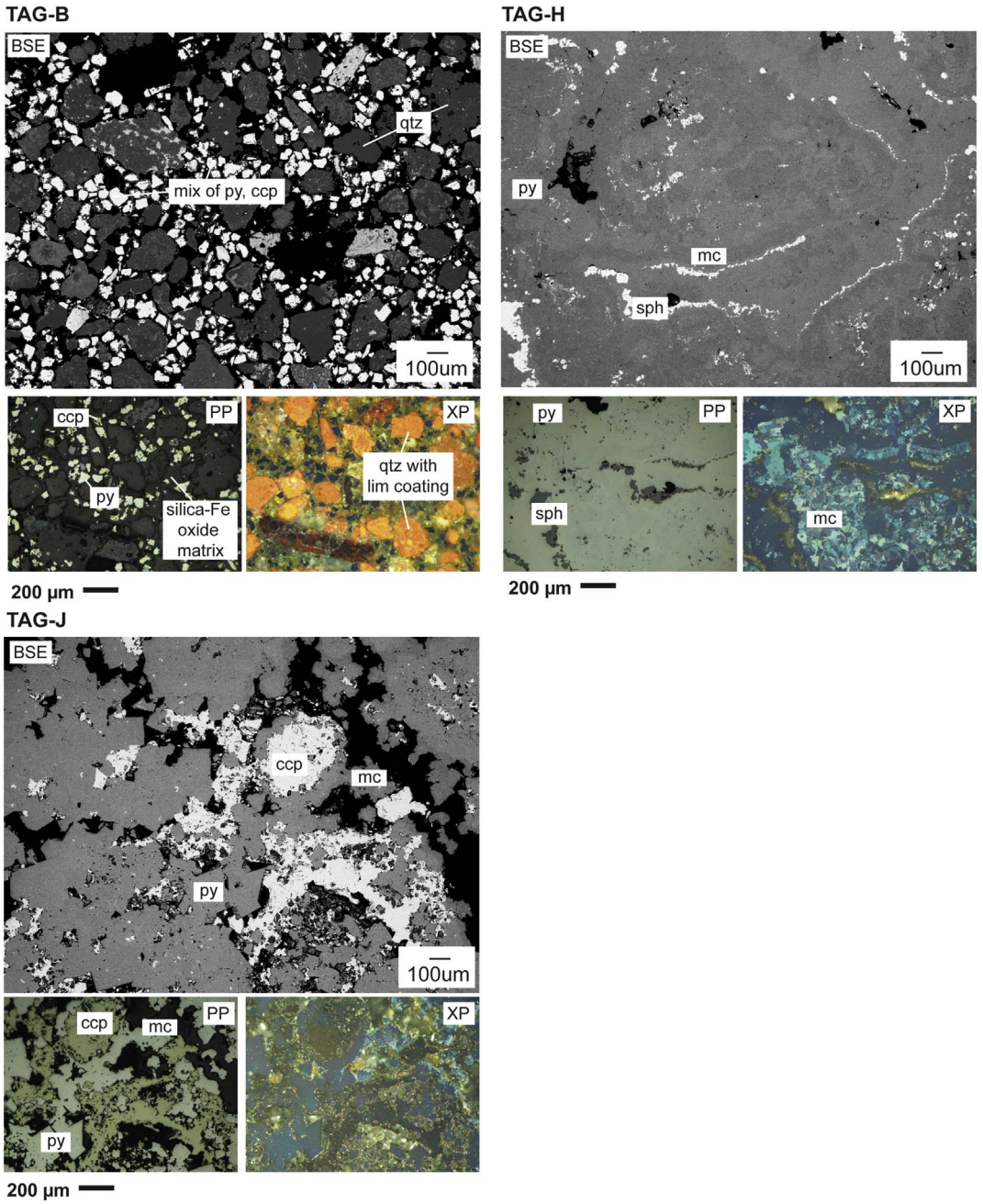

Fig. 3. Back-scattered electron (BSE) and reflected light microscopy photographs (PP, plane polarised; XP, cross polarised) of samples. TAG-B is a heavily oxidised, brecciated sample containing a high abundance of quartz, largely coated in silica and oxidation products including Fe oxides and Fe oxy-hydroxides (limonite). Included in this are grains of pyrite and chalcopyrite, with rare sphalerite. TAG-H is dominantly pyrite and marcasite with sphalerite veinlets and inclusions. TAG-J is similar with major pyrite and marcasite (less marcasite than TAG-H), however contains major chalcopyrite and no sphalerite. *py*, pyrite; *ccp*, chalcopyrite; *mc*, marcasite; *sph*, sphalerite; *qtz*, quartz.

between sulphide powders (due to grain size and/or mineralogy) and allows for normalisation of results. The surface area of all cleaned size fractions were determined using the Brunauer, Emmett and Teller (BET) multiple point N_2 surface area method, on a Quantachrome NOVA 1200 and are quoted in Table 1.

4. Experimental methods

Seawater solutions were made according to the recipe of Millero (2013). They were found to contain on average 391.96 ± 27.66 ppb Fe, 172.63 ± 39.16 ppb Cu and 73.85 ± 19.41 ppb Pb as contaminants. Approximately 0.6–1 g (dependent on availability) of natural TAG sulphide material of 2.5–45 µm was added to 500 mL of seawater. Conductivity, pH and dissolved oxygen (DO) readings were taken throughout the experiments using a HACH meter. Conductivity was calibrated at 12.85 and 53.0 mS cm^{-1} and pH measurement was calibrated at 4.01 and 9. All experiments were stirred using a magnetic flea, the rate of stirring was chosen so that particles remained suspended, analogous to a dewatering of the ship-board ore in a mining context. Temperatures were held at approximately 12 ± 1 °C (simulating the sea surface) using a refrigeration unit. Dissolved oxygen concentrations were controlled by varying the ratio of compressed air to nitrogen using sintered flow meters and were held at approximately 9.0 mg L^{-1} across the duration of each experiment. This oxygen concentration is representative of concentrations within proximity of the TAG hydrothermal field, where values in the Atlantic (A05) eWoce

Table 2
Average concentration of Fe, Cu and Pb within pyrite, marcasite and sphalerite. Concentrations determined by laser ablation inductively coupled mass spectrometry (LA-ICP-MS). N refers to number of analyses. For detailed LA-ICP-MS methodology, please refer to Supplementary material B.

Sample	Phase	N	Fe	Error	Cu	Error	Pb	Error
			wt%		ppm			
TAG-B	Pyrite	4	56.90	2.41	461.20	49.83	11.30	0.68
TAG-H	Pyrite	8	54.21	2.07	33.15	3.67	73.34	4.35
TAG-H	Marcasite	8	55.62	1.87	70.75	4.79	113.59	10.58
TAG-H	Sphalerite	3	0.79	0.02	1720.70	28.35	212.00	6.01
TAG-J	Pyrite	6	57.34	2.64	715.30	43.48	217.30	15.90
TAG-J	Marcasite	3	57.31	1.59	77.20	5.75	65.70	5.29

database show a range between 8.2 and 8.9 mg L^{-1} with the highest concentration observed at 5 km depth at a temperature of 1.5 °C (Schlitzer, 2000). Features of individual experimental runs are summarised in Table 3.

During each experimental run, trace amounts of sulphide material were lost onto the surfaces of monitoring probes and during sample filtration. In order to account for this, the wastewater was filtered, desiccated and weighed, and the value subtracted from the initial weight, as shown in Table 3.

4.1. Sampling protocol

Dissolution experiments adopted a semi-batch design, as described in Rimstidt and Newcomb (1993) and Salmon and Malmström (2006). Seawater samples (13 mL for metal analysis) were removed using a

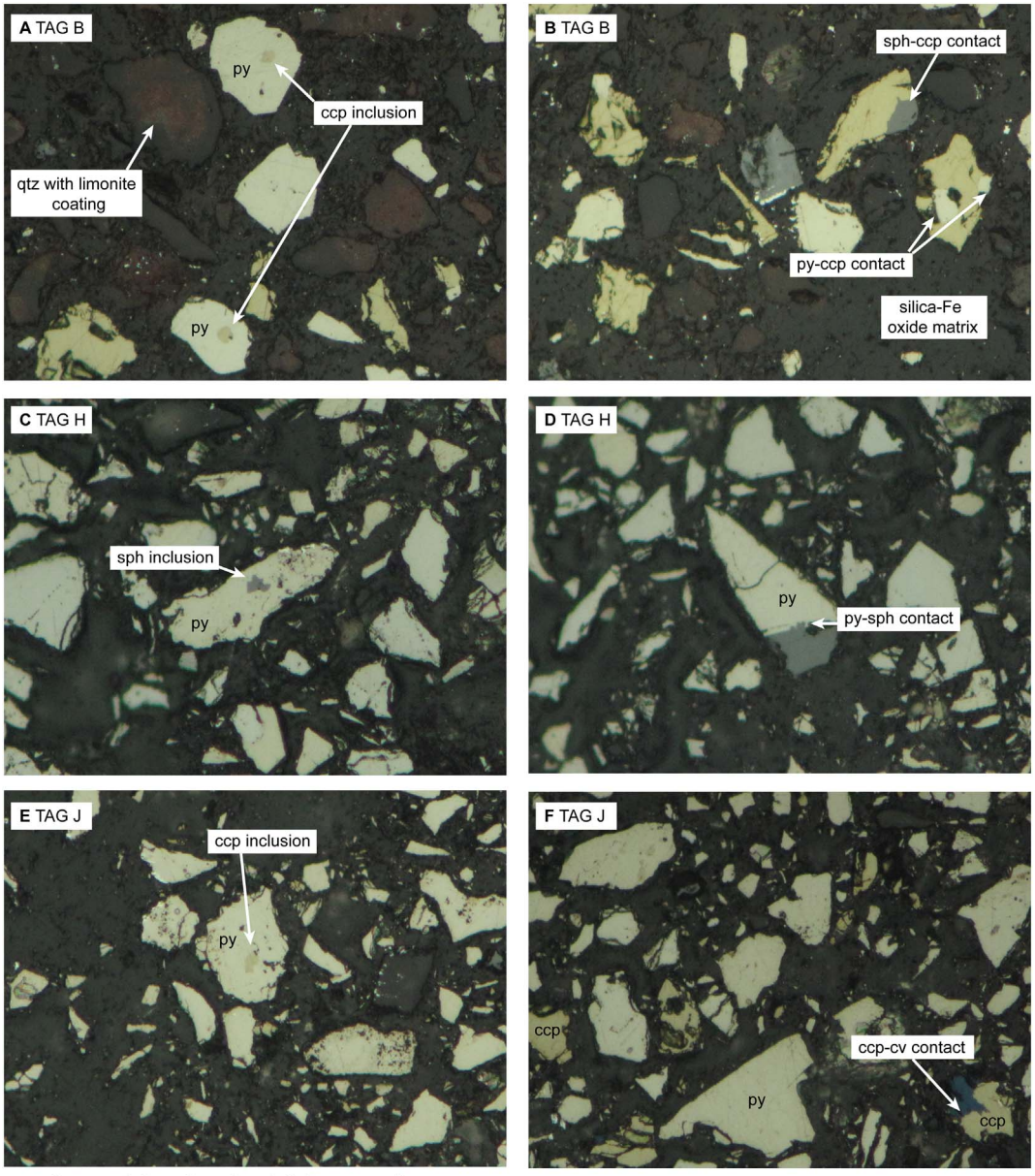

Fig. 4. Reflected light microscope (plane polarised) images of cleaned powders (2.5–45 μm). Presence of inclusions shows their preservation from whole rock sample through the grinding and sieving process. Chalcopyrite inclusions are observed in pyrite grains of both TAG B (top) and TAG J (bottom). Contacts between pyrite-chalcopyrite and sphalerite-chalcopyrite in TAG B and covellite-chalcopyrite in TAG-J are also observed. TAG-H has common sphalerite-pyrite contacts. Whilst inclusions have been identified in grains of the sulphide powders, no quantifiable number can be assigned.

Table 3
Run parameters for experiments conducted in this study. Temperature, oxygen concentration and conductivity are averages of all measurements taken over the course of the run. Dissolved oxygen concentrations were held constant across the duration of experiments. The error reported is the standard deviation between those values.

Run	T	Sample	Size	initial mass	Mass lost on probes	Mass during run	Average dissolved oxygen concentration	Initial pH	Final pH	Conductivity
	°C		μm	g	g	g	mg L^{-1}			mS cm^{-1}
16	11.8 ± 0.6	TAG-B	2.5–45	1.0023	0.0382	0.9641	9.4 ± 0.04	8.05	7.13	37.9 ± 0.2
18	13.0 ± 1.4	TAG-H	2.5–45	0.5939	0.0378	0.5561	9.8 ± 0.70	8.91	7.79	36.5 ± 0.2
19	11.5 ± 1.0	TAG-J	2.5–45	0.9106	0.0682	0.8424	8.96 ± 0.90	8.4	7.56	38.6 ± 0.6

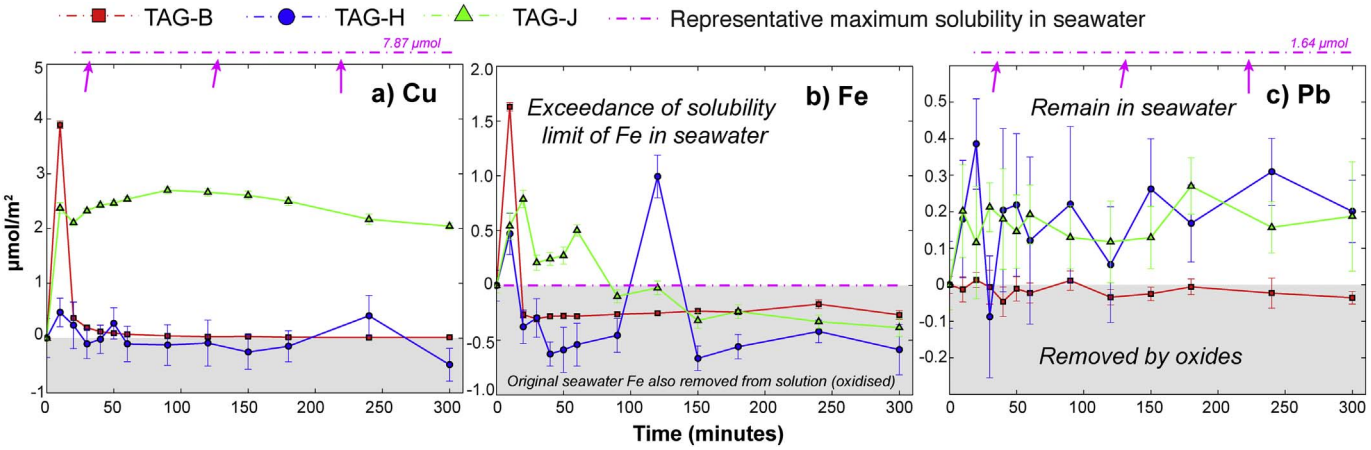

Fig. 5. (a, b and c) Cu, Fe and Pb leached over time with all samples. Concentrations have been corrected to remove initial starting concentrations of Fe, Cu and Pb in seawater and normalised to mass of material, volume of seawater used and surface area of each respective sample and are presented in μmol/m^2. Shown for reference are representative maximum solubility's of Cu, Fe and Pb in seawater taken from experimental and calculation studies (Angel et al., 2015; Franklin et al., 2001; Liu and Millero, 2002). Only Fe exceeds its solubility limit, which is expected based on the pH of the system and is supported by observations of Fe oxide/oxy-hydroxide precipitation.

10 mL mechanical pipette (with an error of 0.5%) for analyses. 13 mL of fresh seawater is added to replace the volume lost at each sampling interval (total of 156 mL over the course of each experiment), with any resultant dilution corrected for (see Section 4.2).

Removed batch samples were filtered using a 0.22 μm pore size to remove all material and halt any further reaction. Sampling occurred every 10 min for the first hour, every half an hour for the following 2 h and every hour up to the full 5 h run time. 5 h run time was chosen to be representative of the amount of time it would take for a steady state to occur between the sulphide and seawater and also reflects the period of agitation related to SMS mining.

Extracted aliquots were analysed using an Agilent 710 ICP-OES. Filtered (0.22 μm) solutions were acidified with 2% HNO_3 in a 2:1 ratio (3 mL sample to 6 mL of nitric acid) to prevent metals from precipitating out and to lower the total dissolved solids to < 1%. All samples were analysed for Fe (234.350), Cu (327.395), and Pb (220.353) with chosen emission lines in brackets. Units of measurement are μg/L, referred to here as ppb. Standards for metals ranged from 1 to 10 ppm. Limits of detection for the ICP-OES for Fe, Cu, and Pb are 0.70, 1.22, and 6.52 ppb respectively.

4.2. Corrections

To account for 13 mL of sample removal and subsequent dilution with 13 mL of fresh seawater, the equations of Salmon and Malmström (2006) were used (Eq. 5). This calculation assumes that elements measured in previous samples remain in solution. The accumulated amount, N, of element j remaining in solution up to sample k, calculated from the measured concentration, C_{meas}, is determined by:

$$N_{k,j} = \left[C_{k,j,meas}\,(V_{0,total} - V_{k,ret}) + \sum_{s=1}^{k} C_{k,j,meas}\,V_{s,sample} \right] \quad (5)$$

All analysed solutions were also corrected for the dilution with nitric acid and initial seawater composition (including removing seawater starting concentrations of Fe, Cu and Pb). These 'corrected' concentrations will henceforth be referred to as 'measured' concentrations.

Measured concentrations were subsequently combined with other data (mass, surface area) in order to highlight the implications for SMS mining. To identify the effect that bulk chemistry and different mineral mixtures (and galvanic effects) exerted on leaching and metals observed in solution, absolute measured concentrations (ppb) require a correction for the variability of sample mass used in each experiment. This correction is outlined in Eq. (1) in Supplementary material E. To assess the potential metal leaching during mining scenarios, absolute measured concentrations (ppb) require a series of corrections including 1) conversion to μmol 2) correction for volume of seawater used and 3) a correction for the sample mass and surface area. These correction procedures are outlined in Eqs. (2) and (3) in Supplementary material E. In this way, results can be extrapolated for leaching outside of the fixed rock to fluid ratio (g/L) using here.

5. Results

Actual measured concentrations and errors (ppb), without corrections for surface area, mass of sulphide material and volume of seawater are presented in Supplementary material F1. However to compare between different samples it is more informative to correct these values to reflect the mass (g) of sulphide material used (Section 5.2) as well as the different available reactive surface areas (Section 5.1).

5.1. Concentrations corrected for mass, volume and surface area (μmol/m^2)

Measured concentrations and errors (ppb) converted to μmol and corrected for surface area, volume of seawater and mass of sulphide material used are presented in Fig. 5, using data produced in Supplementary material F2. Shown for reference are representative maximum

solubilities of Cu, Fe and Pb in seawater taken from experimental and calculation studies (Angel et al., 2015; Franklin et al., 2001; Liu and Millero, 2002). As noted in Fig. 5 and discussed in Section 6, all elements (but particular Fe) may show an increase in the seawater as the metals are leached and/or a decrease as the metals are removed from solution by precipitation of or adsorption onto an oxide.

5.1.1. Cu

All samples show an initial rapid leach of Cu producing a concentration peak measured at the beginning of each experiment but differing in magnitude and time between samples. The maximum concentration peaks for Cu are up to: 3.89 ± 0.07, 0.47 ± 0.26 and 2.37 ± 0.09 μmol/m^2 for TAG-B, H, and J respectively. This initial leach then drops significantly and remains at a more consistent level. After 30 min, the average dissolved Cu was 0.09 ± 0.018, − 0.04 ± 0.33 and 2.41 ± 0.06 μmol/m^2 for TAG-B, H and J. Whilst these are average values, the experiment with TAG-B shows a subsequent slow decrease in aqueous Cu down to 0.01 ± 0.01 (~0 within error). This is in contrast to the experiment with TAG-H where there is overall negligible change in Cu, with only spikes of 0.27 ± 0.28 and 0.41 ± 0.37 μmol/m^2 that are within error of 0 and 0.04 μmol/m^2 respectively. TAG-J is the only experiment where there is an initial leaching of Cu that does not decrease to 0 throughout the 300-minute sampling window. Within this average of 2.37 ± 0.06, there is a peak of 2.69 ± 0.06 μmol/m^2. From the 90 min sampling interval onwards, the amount of Cu dissolved decreases from this peak value but only down to 2.04 ± 0.06 μmol/m^2.

5.1.2. Fe

All samples show an initial leach of Fe to the seawater producing a peak at the beginning of each experiment similar to the observed behaviour of Cu, except here Fe concentrations exceed the solubility limit of seawater. Again, similar to the Cu peak, the magnitude of the Fe peak differs between samples. The initial peaks of Fe are 1.63 ± 0.04, 0.47 ± 0.19 and 0.54 ± 0.12 μmol/m^2 for TAG-B, H and J respectively. This initial dissolved concentration then drops to negative Fe values after the 20-minute sampling interval for experiments with TAG-B and TAG-H and after the 90-minute sampling interval with TAG-J. At the 120-minute sampling interval, TAG-H displays a spike in Fe concentration at 0.99 ± 0.19 μmol/m^2 which does not correspond to either of the Cu spikes of the same experiment.

5.1.3. Pb

The initial peaks of Pb are 0.18 ± 0.16 and 0.20 ± 0.13 μmol/m^2 for TAG-H and J respectively. TAG-B shows negligible leaching initially and throughout the experiment with the exception of small spikes at the 20 and 90-minute sampling interval, which are within error of 0.

In contrast to the behaviour of Cu and Fe in the same experiments, TAG-H and TAG-J show consistent net dissolved Pb throughout the entirety of the experiments. Whilst there are fluctuations during each experiment, there is no overall increase or decrease in the dissolved concentrations of Pb. Across the whole experiment there is an average dissolved concentration of 0.17 ± 0.16 μmol/m^2 and 0.16 ± 0.11 μmol/m^2 of Pb for TAG-H and TAG-J respectively. However, the maximum Pb dissolved throughout the 300 min-sampling interval is 0.38 ± 0.12 μmol/m^2 versus 0.27 ± 0.08 μmol/m^2 for TAG-H and TAG-J respectively.

5.2. Concentrations corrected for mass (ppb/g)

Results presented in μmol/m^2 cannot be used to directly infer the effects of mineral mixtures, as the surface area of the sulphide powder used within the correction for each sample is a summation of the surface area of multiple different mineral phases. Instead, measured concentrations and errors (ppb) corrected for grams of sulphide powder used in each experiment are presented in Fig. 6. Data are presented in Supplementary material F3. Furthermore, data presented in this way can provide an idea of the actual magnitude of dissolved metals when scaled up to ore production quantities.

TAG-J shows the highest dissolved concentration of metals in seawater, on average (from the 30 min sampling interval) 186.01 ± 4.96 ppb Cu per gram of SMS sample and 39.45 ± 26.54 ppb Pb per gram of SMS sample. TAG-H shows similar concentrations of Pb to TAG-J, with an average of 42.78 ± 37.74 ppb per gram of SMS sample after the 30-minute sampling interval.

6. Discussion

SMS material that is disturbed during in situ mining, along with fine particulate SMS materials returned to the ocean after ship-board processing will initially be suspended in the water column as a sediment plume and may be dispersed into the wider ocean, but will ultimately settle out onto the seafloor. Whilst there is still the potential for toxicity and leaching, the in situ extraction is argued to pose less of a risk as a result of the larger grain sizes of the arising particulates (less surface area available for leaching as well as a quicker settling rate, reducing the time the sulphide is exposed for leaching) (Gwyther, 2008). In particular, a study by Bilenker et al. (2016) suggests that acid generation during in situ mining is slow and unlikely to be problematic.

Leaching experiments presented in this study are most representative of the dewatering process during ship-board processing and return of material to the sea, where finer particles are exposed to seawater. During exposure there is potential for these fine sulphide particles to experience more substantial dissolution and release of heavy metals, both locally or some distance into the open sea. Quantification of the distal extent of such plumes and subsequent leaching is difficult to speculate upon without modelling of site-specific plume generation. To this end, stochastic hydrodynamic modelling from Gilbert et al. (2008) was used to investigate the impact of discharging return water at Solwara 1, and the results are applicable to experiments here. The modelling involved a range of variables (dilution rates, temperatures) and found that plumes would dissipate and achieve a dilution of 5000 times within 0.6 km from the point of discharge.

Whilst the Gilbert et al. (2008) model demonstrates that the concentration of fine material (< 8 μm) dilutes fairly rapidly with distal extent, the time it will take for it to fall to the seafloor (and out of the water column) from the designated 25 to 50 m height above the seafloor is not stated. Gilbert et al. (2008) state that over the lifetime of the mining operation (20 months), the peak bottom thickness from the settling fine material is < 0.1 mm. Based on assumptions made in the modelling as applied to the EIS and using Stokes Law, an 8 μm pyrite particle (density of ~5 g/cm^3) would take 1.87 days to settle out from a height of 50 m. However, a 0.1 μm pyrite particle, would take 12,010 days to settle from a 50 m height above the seafloor. Without a better understanding of the grain size distribution within the < 8 μm size bracket, it is difficult to quantify the amount of time sulphide material will ultimately persist and leach in the water column. Furthermore, even after any fine material has settled, whilst the surface area exposed has been reduced, there is still potential for further leaching of metals as the material lies as a poorly consolidated seafloor deposit.

The experiments of this study simulate the consistent stirring of sediments and as a result, the sulphide material has the maximum exposure for leaching. This is representative of the early dissolution process that will occur prior to settling or dilution, especially in the finer fraction. The key processes that control the dissolved concentrations of Fe, Cu and Pb observed include the dissolution rates of all mineral phases, galvanic cells between sulphide minerals grains (sulphide inclusions within grains and/or contacts; Fig. 4, Table 1) that can affect the dissolution rate of particular phases, the formation of any weathering products (Fe oxides and oxy-hydroxides, Cu (± chloride/carbonate) hydroxides in this context) and adsorption of metals onto

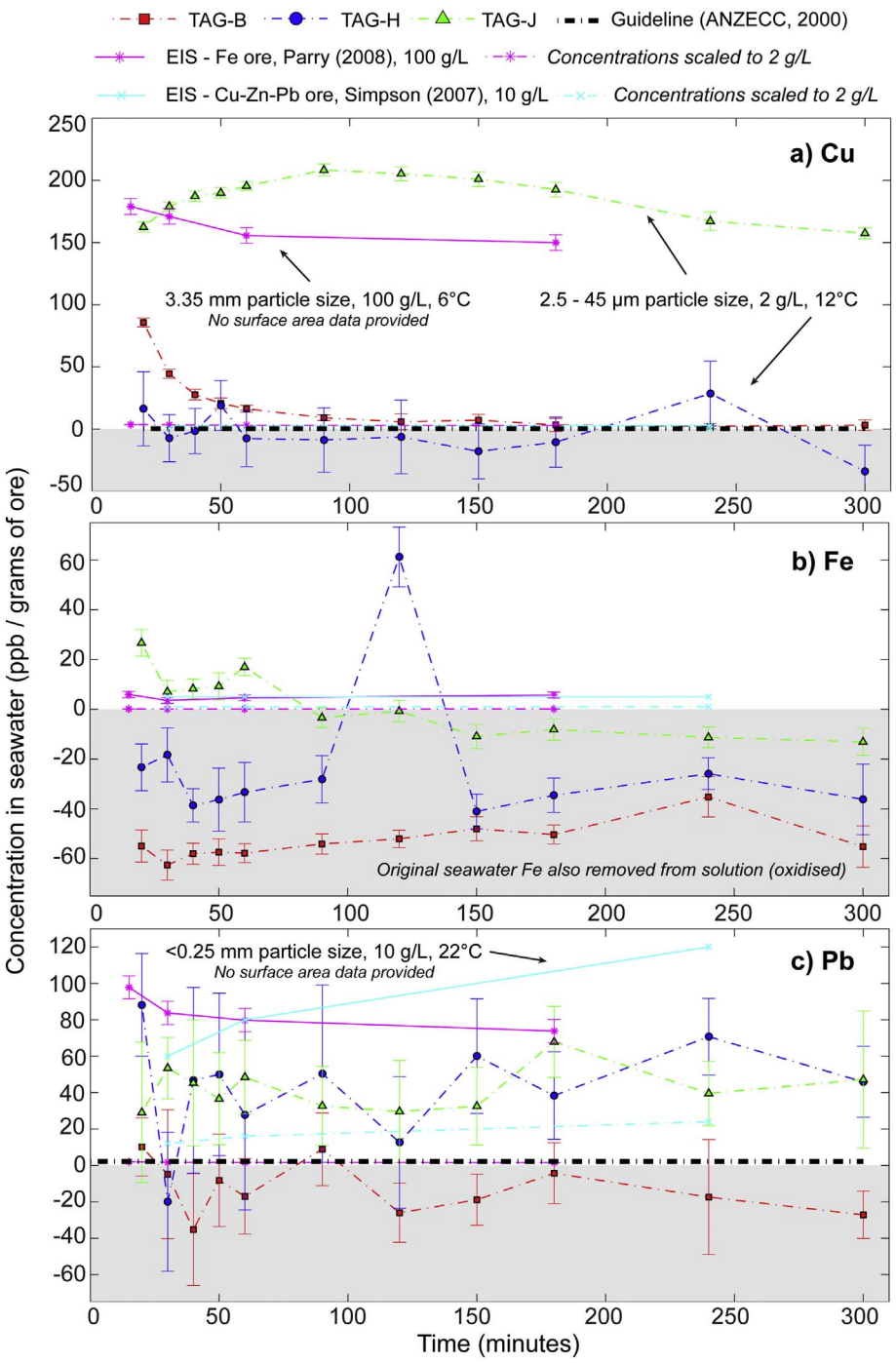

Fig. 6. (a, b and c) Cu, Fe and Pb leached over time with all samples. Concentrations have been corrected to remove initial starting concentrations of Fe, Cu and Pb in seawater and have been normalised to mass of each respective sample and are presented in ppb. Shown for comparison is elutriate data produced by Nautilus Minerals for the EIS (Parry, 2008; Simpson et al., 2007). Pink stars are data from an experiment undertaken with 'representative' Fe-rich Solwara 1 sulphide at 6 °C, particle size of 3.35 mm and a fluid to rock ratio of 25 g to 250 mL (100 g/L) of seawater (Parry, 2008). Cyan crosses are data from an experiment with a Cu-Zn-Pb rich sulphide at 22 °C, particle size of < 0.25 mm and a fluid to rock ratio of 1.25 g to 125 mL (10 g/L) of seawater (Simpson et al., 2007). Solid lines represent absolute concentrations and dashed lines represent concentration (ppb) data scaled to 2 g/L (sulphide material to seawater ratio) for comparison with experiments undertaken in this study. No corrections can be made to scale EIS concentrations for temperature and grain size in order for comparison with this study. (For interpretation of the references to colour in this figure legend, the reader is referred to the web version of this article.)

weathering products present in solution. Based upon the pH (> 7), and concentrations of Cu and Pb observed, the only thermodynamically favourable weathering products in this context are Fe oxides and oxyhydroxides, and due to the experimental design where oxygen was kept constant, are guaranteed throughout the course of all experiments. Cu and Pb concentrations are not high enough to achieve saturation of Cu $(OH)_2$ and $Pb(OH)_2$ and conditions (pH, dissolved concentrations, oxygen, temperature) are not favourable for the formation of other secondary products including atacamite, Cu-ferrite ($CuFe_2O_4$), delafossite ($CuFeO_2$), Pb sulphates and carbonates (Bonatti et al., 1976; Hannington, 1993; John et al., 2016; B., 1978; Kolta et al., 1981; Ridley, 2012; Swallow and Morel, 1980; Taylor, 2011).

Fig. 7 demonstrates the average dissolved metal as a proportion of the bulk concentration, expressed as a percentage. Whilst percentage dissolved values are in themselves small, it is important to note the high bulk concentrations of heavy metals in the TAG samples; making this small loss significant in terms of toxicity. Within the first 10 min, TAG-H demonstrates the highest initial percentage loss of Cu and Pb, whilst TAG-B shows a high loss of Cu and TAG-J a loss of Pb.

Using the data of this study as a 'realistic' example (although this ignores any biological effects), these results suggest that a total of 0.04 and 0.002 wt% of Cu, Fe and Pb will be leached from a deposit such as TAG-H and TAG-B respectively, at the initial stages of processing (Fig. 7). However, with both experiments, the decrease of Fe to negative values (below initial seawater background) is consistent with the precipitation of Fe oxides and exceedance of the solubility limit of Fe in seawater (Fig. 5). Furthermore, the removal of Cu from solution from both experiments after 10 min, suggests that the Fe and Cu leaching

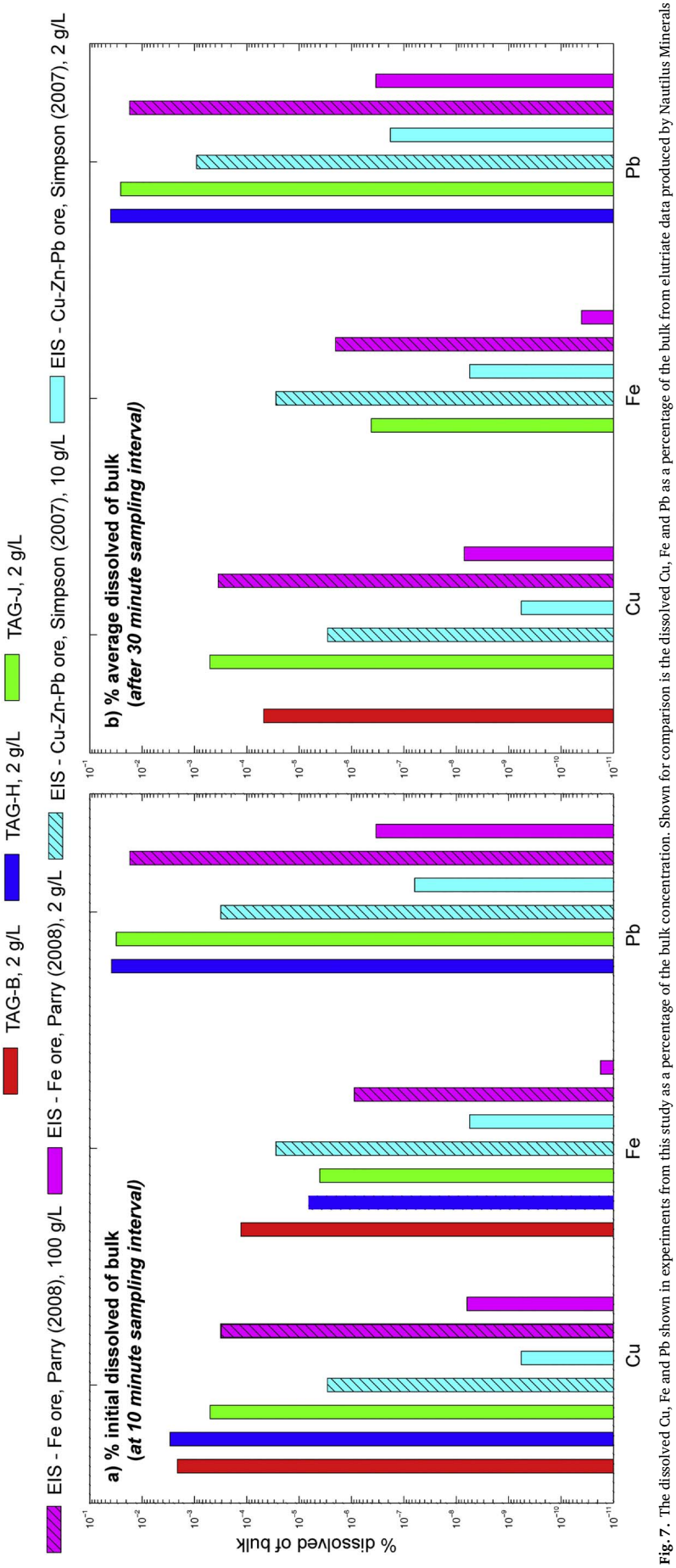

Fig. 7. The dissolved Cu, Fe and Pb shown in experiments from this study as a percentage of the bulk concentration. Shown for comparison is the dissolved Cu, Fe and Pb as a percentage of the bulk from elutriate data produced by Nautilus Minerals for the EIS. Hatched bars indicate concentrations that have been corrected to 2 g/L rock to fluid ratio, in line with this study. a) Initial loss of bulk as a %, at the 10-minute sampling interval. b) Dissolved concentrations as a % of the bulk, taken as an average after the 30-minute sampling interval.

potential of deposits such as TAG-H and TAG-B will be reduced even more when dilution subsequently occurs.

A deposit such as TAG-J is more concerning. 0.03 wt% of Cu, Fe and Pb will be lost in the initial stages of processing (Fig. 7a), but leaching of Cu and Pb will continue (Fig. 7b) until either the particle interface has been fully dissolved or an oxide forms on the particle surface and insulates it from the seawater (passivation on the surface, which is expected in most cases). However, the fact that precipitation of oxidation products and adsorption onto oxidation products is not shown to remove the sustained dissolved metals for TAG-J is a cause for concern. In the TAG experiments where a loss is observed, Pb and Cu have the highest percentage dissolved, indicating their higher propensity to be leached and stay in solution compared to Fe. This is also observed in experiments undertaken in the EIS (see Fig. 7) and expected as a result of the higher solubility limits of Cu and Pb in seawater in comparison to Fe.

Whilst all three TAG samples contain similar concentrations of Pb (100–200 ppm, Table 1), it is only TAG-H and TAG-J that show leaching of Pb into seawater (both at ~40 ppb). Similarly, TAG-B, a sample that contains a similar total amount of chalcopyrite and bulk Cu as TAG-J (Table 1), shows initial leaching of Cu (Fig. 5), but this is removed after 30 min in contrast to TAG-J. This indicates that the leaching of Cu from TAG-J is at a higher magnitude than any removal through oxidation (due to mineralogy or galvanic effects) and that the method of removal of Cu and Pb from TAG-B is different to TAG-J and TAG-H (due to mineralogy). This is discussed further in Section 6.1. Either way, the leaching results demonstrate that bulk chemistry does not dictate the concentration of metals dissolved into seawater. Instead, mineralogy and/or possible galvanic effects are the driving forces behind the type and concentration of metals remaining in seawater after leaching.

As shown in Fig. 6a, b and c, the high concentrations of Fe and Cu dissolved in experiment TAG-J are very similar to those observed in experiments from the EIS. The figure shows results from two different published experimental datasets that have the most similar run conditions to those used in the current study. The specific mineralogy of the samples used within the EIS was not presented for either the experiments of Parry (2008) or Simpson et al. (2007), although the overall chemistry was provided and is reproduced in Supplementary material A. Based on this chemistry, the mineralogy is substantially different between each of their experiments.

Data from Parry (2008) uses predominantly Fe-rich samples (31.6% Fe, 5.13% Cu, 3670 ppm Zn) similar to our experiments with deposits from TAG (Table 1, bulk Fe and Cu) with Cu and Pb dissolved at similar concentrations as TAG-J, despite a larger grain size, and higher temperature and rock-fluid ratio. Studies by Moses and Herman (1991) and Simpson et al. (2007) indicate a linear relationship between rock to fluid ratio and dissolved metals, allowing for data to be scaled to take into consideration the difference in rock-fluid ratio between studies. When data from Parry (2008) is scaled to the rock-fluid ratio used in this study (2 g/L), concentrations drop to ~3 ppb for Cu and ~2 ppb for Pb. This lower concentration/lower percentage loss of bulk observed in the EIS data when scaled to 2 g/L (Figs. 6 & 7) can be explained by the larger grain size (less surface area) used in their experiments. The massive sulphide used in experiments by Simpson et al. (2007) has significantly higher bulk Cu, Zn, Pb and As than massive sulphide used by Parry (2008) and the TAG samples used here (Supplementary material A). Despite this, the dissolved Cu and Pb is much lower than the comparable experiments with Fe-rich massive sulphide as shown in Fig. 7. This is comparable to our results, where bulk chemistry does not define the metals that are leached and remain in solution.

Based on the effect that differing mineralogy has on the leaching of massive sulphides presented in this study, it is imperative that extensive tests with the full range of mineralogy and geochemistry of ore mined are undertaken prior to any future mining of a deposit. Results where only one type of ore are utilised in experiments are applicable to only a particular area of a deposit and are not ubiquitously transferable.

6.1. The effect of mineralogy on leaching and dissolved metals

By combining the observed mineral proportions and bulk chemistry from Table 1 with the magnitude of metal released to the seawater (ppb), corrected for grams of material tested (Fig. 6), it should be possible to at least speculate on the effect that mineralogy, texture and possible galvanic reactions might have on the 'leaching' process. It must be remembered that the 'leaching' simulated here and in particular the monitoring of metal release with time as sulphide minerals dissolves, will be counteracted by subsequent oxide precipitation in these experiments. The measured metals in solution can only give a net view of the two competing processes.

In addition to the new Fe-oxide precipitation, some massive sulphide samples such as TAG-B initially contain a high proportion of Fe oxides and oxy-hydroxides (Fig. 3, Table 1) that would represent a large surface area of the processed material, and will be present at the beginning of our leaching experiments. This could represent either a source to release metals or remove them in a similar way to the newly formed Fe precipitate. In the latter case, the presence of Fe oxides/oxy-hydroxides within the deposit prior to mining (likely in the case of an inactive SMS deposit) could be advantageous in reducing the environmental toxicity associated with mining.

All three TAG samples contain similar Pb concentrations (100–200 ppm), yet only samples TAG-H and J show leaching. No galena or major Pb bearing minerals were identified in the samples, indicating that the Pb must arise from the lattice sites of sulphide phases (Table 2), though it is not possible to identify the particular mineral phase contributing the Pb from these data alone. The observation that TAG-B has negligible Pb dissolved whilst demonstrating similar bulk Pb suggests that Pb is present as a phase that is not leaching or is more stable (e.g. sorbed onto present Fe oxy-hydroxide).

Based on bulk analysis alone (Table 1), it might be expected that TAG-B would demonstrate the highest Cu release and concentration in the seawater. Whilst it does leach the highest initial concentration of Cu (Fig. 5), it is TAG-J that maintains the higher dissolved Cu throughout the 300-minute experiment. It is clear from the TAG-J experiment that the formation of weathering products and their adsorption capacity does not keep up with the leaching of Cu, resulting in consistently high dissolved Cu. The disparity between TAG-B and J can ultimately be explained by either 1) a different Cu host/source, 2) a difference in mechanism leaching Cu, 3) a difference in mechanism removing Cu or 4) a difference in exhaustion/isolation (passivation) of Cu host/source. These possibilities are discussed in further detail below.

6.1.1. Hosts and sources of Cu

Chalcopyrite is the largest source of Cu observed in both TAG-B and TAG-J (5.2 and 4.7 wt% respectively). The marginally higher abundance of chalcopyrite could explain the higher initial leach of Cu observed in TAG-B over TAG-J. In reality, chalcopyrite has been shown to have at least an order of a magnitude slower dissolution rate than both pyrite and marcasite (Bilenker, 2011; Feely et al., 1987; Romano, 2012), which are host to Cu at trace levels in the mineral lattice (Table 2). Based on comparison of abundance of marcasite, trace Cu in marcasite between TAG-H and TAG-J (44.3% vs 5.8% respectively, ~70 ppm, Tables 1 and 2) and dissolved concentrations of Cu, marcasite can be ruled out as a source of the Cu observed in TAG-J. Pyrite on the other hand, could be a plausible source to explain the disparity between TAG-B and J when considering its high concentrations of trace Cu (715.30 ppm) and abundance in TAG-J (four times that of TAG-B), however this does not explain the high initial release observed in TAG-B.

Another plausible Cu source to consider and explain the disparity between TAG-J and TAG-B, would be secondary formed Cu sulphide minerals. TAG-J was shown to contain rare covellite (CuS) during

reflected light microscopy and XRD analysis at ~1.4 wt%. Covellite has been demonstrated to have higher dissolution rates than chalcopyrite, but how this rate compares to pyrite and marcasite is unknown (Fullston et al., 1999). The leaching of covellite could provide a tenuous explanation for the heightened dissolved Cu in TAG-J over TAG-B, but still does not explain the higher initial leach of Cu during the TAG-B experiment. The presence of atacamite in TAG-B (3.9%, Table 1) does provide another Cu source, and according to the solubility and dissolution rate of atacamite in seawater and NaCl solutions at a range of pH (Hannington, 1993; Le Roux et al., 2016; Pollard et al., 1989; Savenko and Shatalov, 1998), could also account for the higher initial release observed.

The observation of dissolved Cu decreasing throughout the experiment with TAG-B could suggest exhaustion of a Cu source or its isolation from the seawater. However, it would be difficult to explain why any reduction in availability is occurring throughout the experiment in TAG-B and not TAG-J based on the constant dissolved oxygen concentrations.

Adsorption onto Fe oxides and oxy-hydroxides observed in TAG-B (19.5%, Table 1; Fig. 3) could account for the subsequent drop in Cu over time observed during the experiment with TAG-B (Fig. 5). New oxide phases that form throughout the TAG-J experiment are unlikely to provide as high of a surface area for adsorption as the already established oxides present in TAG-B do based on the high abundance observed. If this is the case, the presence of Fe oxides/oxy-hydroxides within the deposit prior to mining (likely in the case of an inactive SMS deposit) could be advantageous in reducing the environmental impact associated with mining.

6.1.2. Galvanic cells

In terms of alternative causal effects, galvanic cells have been shown to significantly increase dissolution (Abraitis et al., 2004a; Heidel et al., 2013; Koski et al., 2008; Kwong et al., 2003; Li et al., 2006; Liu et al., 2008). Whilst it is unlikely that any separate grains would be able to stay in contact for long enough to create a cell in these stirred experiments, individual particles composed of multiple sulphide phases can create a cell with seawater. Sulphide minerals within both TAG-B and TAG-J contain sulphide inclusions in whole rock samples and cleaned massive sulphide powders (some < 1 μm) of chalcopyrite in pyrite/marcasite grains and vice versa (see Figs. 3 and 4), allowing galvanic cells the ability to form during leaching experiments. In this scenario, the lower potential of chalcopyrite (Fig. 1) would cause it to be preferentially dissolved relative to pyrite (or marcasite), releasing Cu and some Fe into solution.

TAG-B has much less pyrite than TAG-J (19.7% vs. 84.2% pyrite plus 5.8% marcasite), and consequently, fewer inclusions to allow for galvanic cells to occur. If galvanic cells were playing a role, it would be expected that both TAG-B and TAG-J would display a leach of Cu, just at a higher magnitude in TAG-J, which is not observed in the initial leach (TAG-B has a higher initial leach). However, this could be easily explained by an initial leach of chalcopyrite in both that slows with time (producing the higher initial leach of Cu in TAG-B), with galvanic cells in TAG-J producing the higher dissolved Cu concentrations observed later on.

Exact quantification of the extent to which galvanic coupling, and mineralogy (and any associated adsorption) is contributing to dissolution role is not possible within the scope of this study, simply because there are numerous inseparable variables at play. Nonetheless their impact on the leaching of SMS needs to be considered and accounted for in environmental impact predictions.

6.2. Toxicity potential

The toxicity induced by sulphide dissolution may have some detrimental impact on the environment around SMS deposits and associated ecosystems, although this will ultimately be highly variable. It has been speculated that any high concentrations of heavy metals that are leached or present in the plume will pose minimal risk to a faunal system already adapted to active SMS deposits (Simpson et al., 2007; Gwyther, 2008; Parry, 2008; Sander and Koschinsky, 2011). However the most distal 'background' fauna may not have developed such survival strategies. Furthermore, if mining occurs at inactive SMS deposits where adaptation to toxicity is lower, the impact to this specific ecosystem may be more significant; unless these ecosystems have a high recovery rate.

Initial high metal concentrations (within 10 min) are unlikely to cause serious problem for fauna as they are quickly removed (presumably via precipitation of oxides and adsorption onto oxides), with suffocation from plumes a more serious concern in the initial stages. Whilst the average percentage loss (Fig. 7) is very small across all metals and samples (< 0.1%), the sustained dissolved metals at a ppb level is still considered significant due to their exceedance of both Australian and New Zealand water quality (ANZECC) and UK Marine Special Areas of Conservation (SAC) environmental guidelines. It is difficult to apply these guidelines to black smoker environments, where background toxicant concentrations vary significantly and the ecosystems are dramatically different to 'normal' marine ecosystems. In fact, no guidelines exist for such environments. For purposes of discussion and to compare experiments undertaken here with those undertaken in the EIS for Solwara-1, the minimum guideline for each metal has been chosen (99% protection, ANZECC). Guidelines are 0.3 and 2.2 ppb for Cu and Pb respectively.

Based on the current mining concept outlined by Nautilus Minerals for their EIS, the return water will include solid material < 8 μm in diameter with an expected total dissolved solids (TDS) of 6.35 g/L (Gwyther, 2008) compared to the 2 g/L of this study. When experiments in this study are scaled to the rock-fluid ratio outlined in the EIS (Supplementary material G), Cu concentrations observed for TAG-J would increase to an average of 590.6 ± 15.7 and Pb concentrations to 133.4 ± 84.8 ppb. TAG-H's Pb concentrations would increase to an average of 135.8 ± 119.8 ppb. These are well above guidelines before dilution is taken into consideration.

Based on experiments with 2 g/L, TAG-J would require 620 times dilution to reduce Cu concentrations to within the 0.3 ppb ANZECC guideline. When scaled to the expected 6.35 g/L rock to fluid ratio, a 1968 times dilution would be required during mining. For TAG-H at 2 g/L, a 19.4 times dilution would be required to bring the Pb concentration in line with the 2.2 ppb UK-SAC guideline. This would increase to 61.7 times if scaling the concentrations to the 6.35 g/L ratio. Elutriate experiments undertaken by Simpson et al., 2007 find that dilutions of > 4000 times may be necessary for samples from Solwara, double the values suggested by this study. The higher dilution requirement is likely to accommodate the high observed concentrations of As and Zn in their dataset, elements which were not considered in this study. Whilst it is likely that As and Zn are present in higher concentrations at Solwara than the TAG samples used here, data from Solwara experiments and trace element studies (e.g. Hannington et al., 1991 and Wohlgemuth-Ueberwasser et al., 2015) suggest that As, Zn, Co and Cd could be leached during mining, and thus will require further investigation.

If the 2 g/L rock to fluid ratio is kept constant, localised toxicity would be expected in a stagnant water column. However, in reality, dilution is expected where both plumes created by dewatering or extraction and deep-sea currents have the ability to entrain fresh seawater. Hydrodynamic modelling can give an indication of dilution of heavy metal concentration with distance but is site specific and does not take into consideration the time it would take for dilution to occur. Gilbert et al. (2008) demonstrate a 600-fold volume dilution would be achieved within 85 m of the point of discharge at Solwara-1. However if TAG dissolved metal concentrations of this study were scaled to 6.35 g/L, a 2000 fold volume dilution is required which would only be achieved at 600 m from the discharge. Ultimately, the distance at which

dilution is achieved to meet guidelines may not be sufficient, indicating either the potential need for ship-board dilution prior to the return of waste water or refinement of the mining process. Of more concern is that this does not include any sulphide mineral particulate remaining in the diluted seawater volume, which may continue to release further metals to solution during any dilution process.

In terms of total input into the ecosystem, the EIS for the proposed Solwara-1 deposit in Papua New Guinea currently suggests a footprint of approximately 0.112 km^2 will be mined over five mineralised areas. If an area of that size at TAG was to be mined and was identical in mineralogy, bulk chemistry and texture to TAG-J, there would be a cumulative total of 0.0224 mol of Cu (14,230 ppm) added to the seawater throughout the mining project.

Application of the data from this study and the Solwara-1 EIS might be 'conservative' given that a finer size fraction (< 8 μm) is planned for the discharge of return water. This small size would result in a significantly higher surface area and higher leaching rate. The potential for toxicity during dewatering would be far more substantial than observed during the course of these experiments. In addition, there are SMS deposits that are known to contain considerably higher concentrations of toxic metals (As, Pb, Sb, Zn, Co, Cd, Ni and Hg) than TAG (e.g. mafic-hosted, felsic-hosted, young, back-arc basin settings (Herzig and Hannington, 1995)), further increasing the potential for environmental impact.

Finally, it is widely accepted that Fe-oxidising bacteria play a significant role during the weathering (oxidative dissolution) of seafloor massive sulphide deposits (Edwards et al., 2003). Rimstidt et al. (1994), Plumlee et al. (1999), Corkhill (2008) and Koski et al. (2008), all suggest that redox reactions utilising Fe^{3+} produced by bacteria catalyse reaction rates of sphalerite, chalcopyrite, enargite and arsenopyrite. Lizama and Suzuki (1991), show that *Thiobacillus ferroxidans* and *Thiobacillus thiooxidans* both increase the leaching rates from sulphide minerals (pyrite, chalcopyrite, sphalerite) by up to 44.2% in some cases. It has also been reported in numerous dissolution studies (Ahonen et al., 1985; Berry et al., 1978; Jyothi et al., 1989; Mehta and Murr, 1982, 1983, Natarajan, 1985, 1988, Natarajan and Iwasaki, 1983, 1986; Yelloji Rao and Natarajan, 1989) that the presence of bacteria such as *Thiobacillus ferroxidans* in a polymetallic sulphide mixture can accelerate galvanic interactions significantly. Whilst the role of microbes is highly important in the longer-term, in-situ, natural oxidation of seafloor massive sulphide deposits, it has been suggested that abiotic oxidation rates of sulphide minerals are more relevant to the oxidation of sulphides during seafloor mining (Bilenker et al., 2016; McBeth et al., 2011). It is postulated that bacterial colonization of freshly ground mineral surfaces is unlikely under the rapid time spans of mining (< 30 min based on mining scenarios outlined by Nautilus Minerals Inc. However biotic oxidation could be of significant concern once fine sulphide material has settled after initial extraction and dewatering. Leaching of metals has the potential to continue after material has settled, not only abiotically but also when bacteria colonise the high surface area of sulphide material that has been exposed due to mining.

7. Conclusions and future directions

Experiments presented here at 1 atm and 12 °C with SMS samples from TAG, Mid Atlantic Ridge show a dissolved concentration of metals (primarily Cu and Pb) at the parts per billion range that is not balanced by removal (e.g. by precipitation and/or adsorption over time. Quantifying the extent to which factor such as galvanic coupling, and mineralogy (and any associated adsorption) or even biotic processes contribute to dissolution rates is not possible within the design of this study, but will need to be assessed in future studies. Nonetheless, the results of this study clearly demonstrate that the complexity surrounding the leaching of SMS deposits needs to be considered and accounted for in environmental impact predictions. A combination of this study with analysis of the precipitated material would be a first step in advancing our understanding. It is also worth noting the higher pressure involved on the seabed.

The evidence presented here clearly demonstrates that bulk chemistry alone cannot dictate the concentration of metals leached into seawater. Instead, a combination of mineralogy, adsorption processes and/or galvanic effects must be considered as the primary driving forces behind the type and concentration of metals released and removed into the water column during SMS mining. As a result, it is imperative that extensive tests with the full range of sulphide mineralogy from future prospect sites are undertaken prior to activation of any extraction activities. Results where only one type of massive sulphide are utilised in experiments are applicable to only a particular area of a deposit and are not ubiquitous. Furthermore, results of the study suggest that the presence of Fe oxides/oxy-hydroxides within the deposit prior to mining (likely in the case of an inactive SMS deposit) could be advantageous in reducing the environmental toxicity associated with mining. The full contribution of galvanic coupling on the leaching of SMS deposits remains unclear and observation of dissolution and oxidation in situ using atomic force microscopy (AFM) experiments could help to advance our understanding of galvanic couples between specific mineral combinations.

In these experimental simulations, dissolved concentrations exceed the 99% protection, ANZECC toxicity guidelines by 620 times, and would imply the formation of localised toxicity in a stagnant water column. In reality this concentration will most likely be rapidly diluted by the entrainment of fresh seawater as a result of plume mixing (during the mining process) and/or deep ocean currents (site specific). Nevertheless, the distance at which dilution is achieved to meet guidelines is unlikely to be sufficient, indicating either a potential need for ship-board dilution prior to the return of waste water or a refinement of the mining process. Dilutions required to meet toxicity guidelines (for Cu and Pb) when mining a deposit like TAG, are less than half of those required for a deposit like Solwara 1 and imply that a deposit such as TAG could pose less of a risk to mine (in terms of leaching and toxicity) than Solwara 1. However, it should be noted that concentrations will be much higher compared to these experiments when scaled to more realistic rock-fluid ratios and a finer grain size (< 8 μm) as proposed for seafloor mining scenarios.

SMS deposits that contain higher concentrations of Cu and Pb than TAG, as well as other heavy metals in higher abundance (e.g. mafic-hosted and felsic-hosted (young, back-arc basin) settings (Herzig and Hannington, 1995)) signify an elevated risk of leaching when considering their environmental impact during the mining process (smaller grain size and higher rock-fluid ratio). This study highlights the importance of further research to predict and mitigate the effects of imminent SMS mining.

In order for deep-sea mining to take place in the future, the environmental impact of such an undertaking needs to be fully understood and demonstrated. Experiments highlighted here and future planned experiments can help refine the mining processes and minimise detrimental impacts by providing recommendation of grain size fractions and rock-fluid ratios that can be adopted to reduce any risk of leaching and toxicity. Furthermore, certain types of deposit or mineralogies can be identified as presenting more or less of a risk. This can ensure minimal leaching of heavy metals and a reduction of environmental impact.

Supplementary data to this article can be found online at https://doi.org/10.1016/j.marpolbul.2017.10.079.

Acknowledgements

We would like to thank the Engineering and Physical Sciences Research Council (EPSRC) and Ascension Holdings Ltd. (AHL) for financially supporting this research. We would also like to thank ODP for kindly providing TAG samples that allowed for this study to take place.

A huge thanks to Sven Petersen and Matthias Frische who provided considerable assistance with collection and processing of LA-ICP-MS data at GEOMAR Helmholtz-Zentrum für Ozeanforschung, Kiel. Dieter Garbe-Schönberg and Ulrike Westernströer provided much help and guidance with the digestion and analysis of the TAG samples at the University of Kiel.

References

Abraitis, P., Pattrick, R.A.D., Kelsall, G.H., Vaughan, D.J., 2004a. Acid leaching and dissolution of major sulphide ore minerals: processes and galvanic effects in complex systems. Mineral. Mag. 68, 343–351. http://dx.doi.org/10.1180/0026461046820191.

Abraitis, P., Pattrick, R.A.D., Vaughan, D.J., 2004b. Variations in the compositional, textural and electrical properties of natural pyrite: a review. Int. J. Miner. Process. 74, 41–59. http://dx.doi.org/10.1016/j.minpro.2003.09.002.

Acero, P., Cama, J., Ayora, C., Asta, M.P., 2009. Chalcopyrite dissolution rate law from pH 1 to 3. Geol. Acta 7, 389–397. http://dx.doi.org/10.1344/105.000001444.

Ahmad, R., Kumar, R., Haseeb, S., 2012. Adsorption of Cu2+ from aqueous solution onto iron oxide coated eggshell powder: Evaluation of equilibrium, isotherms, kinetics, and regeneration capacity. Arab. J. Chem. 5, 353–359.

Ahonen, L., Hiltunen, P., Tuovinen, O., 1985. The role of pyrrhotite and pyrite in the bacterial leaching of chalcopyrite ores. In: Branion, R.M.R., Ebner, H.G. (Eds.), Fundamental and Applied Biohydrometallurgy, pp. 13–22 Amsterdam.

Angel, B.M., Apte, S.C., Batley, G.E., Raven, M.D., 2015. Lead solubility in seawater: an experimental study. Environ. Chem. 13, 489–495.

B., K.W., 1978. The Weathering of Sulfide-bearing Rocks Associated with Porphyry-type Copper Deposits. The University of Arizona.

Balistrieri, L.S., Murray, J.W., 1982. The adsorption of Cu, Pb, Zn, and Cd on goethite from major ion seawater. Geochim. Cosmochim. Acta 46, 1253–1265. http://dx.doi.org/10.1016/0016-7037(82)90010-2.

Benjamin, M.M., Leckie, J.O., 1981. Multiple-site adsorption of Cd, Cu, Zn, and Pb on amorphous iron oxyhydroxide. J. Colloid Interface Sci. 79, 209–221. http://dx.doi.org/10.1016/0021-9797(81)90063-1.

Berry, V.K., Murr, L.E., Hiskey, J.B., 1978. Galvanic interaction between chalcopyrite and pyrite during bacterial leaching of low-grade waste. Hydrometallurgy 3, 309–326. http://dx.doi.org/10.1016/0304-386X(78)90036-1.

Bilenker, L., 2011. Abiotic Oxidation Rate of Chalcopyrite in Seawater: Implications for Seafloor Mining. University of California Riverside.

Bilenker, L.D., Romano, G.Y., McKibben, M.A., 2016. Kinetics of sulfide mineral oxidation in seawater: implications for acid generation during in situ mining of seafloor hydrothermal vent deposits. Appl. Geochem. 75, 20–31. http://dx.doi.org/10.1016/j.apgeochem.2016.10.010.

Bonatti, E., Guerstein-Honnorez, B.-M., Honnorez, J., 1976. Copper-iron sulfide mineralizations from the equatorial Mid-Atlantic Ridge. Econ. Geol. 71.

Bonnissel-Gissinger, P., Alnot, M., Ehrhardt, J.-J., Behra, P., 1998. Surface oxidation of pyrite as a function of pH. Environ. Sci. Technol. 32, 2839–2845. http://dx.doi.org/10.1021/es980213c.

Cheng, X., Iwasaki, I., 1992. Pulp potential and its implications to sulfide flotation. Miner. Process. Extr. Metall. Rev. 11, 187–210. http://dx.doi.org/10.1080/08827509208914206.

Cherkashev, G.A., Ivanov, V.N., Bel'tenev, V.I., Lazareva, L.I., Rozhdestvenskaya, I.I., Samovarov, M.L., Poroshina, I.M., Sergeev, M.B., Stepanova, T.V., Dobretsova, I.G., Kuznetsov, V.Y., 2013. Massive sulfide ores of the northern equatorial Mid-Atlantic Ridge. Oceanology 53, 607–619. http://dx.doi.org/10.1134/S0001437013050032.

CLCS, 2017. Oceans and law of the sea, United Nations. Submissions, through the Secretary-General of the United Nations, to the Commission on the Limits of the Continental Shelf, pursuant to article 76, paragraph 8, of the United Nations Convention on the Law of the Sea of 10 December 1982. Available at: http://www.un.org/depts/los/clcs_new/commission_submissions.htm.

Constantin, C.A., Chiriță, P., 2013. Oxidative dissolution of pyrite in acidic media. J. Appl. Electrochem. 43, 659–666. http://dx.doi.org/10.1007/s10800-013-0557-y.

Corkhill, C.L., 2008. The Mineralogical and Biogeochemical Transformations Associated With As-bearing Sulphide Minerals in Acid Mine Drainage System. The University of Manchester.

Descostes, M., Vitorge, P., Beaucaire, C., 2004. Pyrite dissolution in acidic media. Geochim. Cosmochim. Acta 68, 4559–4569. http://dx.doi.org/10.1016/j.gca.2004.04.012.

ECORYS, 2014. Study to Investigate State of Knowledge of Deep Sea Mining: Final Report: Annex 5 Ongoing and Planned Activity.

Edwards, K.J., 2004a. Special Paper 379: Sulfur Biogeochemistry - Past and Present. Geological Society of America Special Papers Geological Society of Americahttp://dx.doi.org/10.1130/0-8137-2379-5.

Edwards, K.J., 2004b. Formation and degradation of seafloor hydrothermal sulphide deposits. Geol. Soc. Am. Spec. Pap. 379, 83–96. http://dx.doi.org/10.1130/0-8137-2379-5.83.

Edwards, K.J., McCollom, T.M., Konishi, H., Buseck, P.R., 2003. Seafloor bioalteration of sulfide minerals: results from in situ incubation studies. Geochim. Cosmochim. Acta 67, 2843–2856. http://dx.doi.org/10.1016/S0016-7037(03)00089-9.

Fallon, E.K., Petersen, S., Brooker, R.A., Scott, T.B., 2017. Oxidative dissolution of hydrothermal mixed-sulphide ore: an assessment of current knowledge in relation to seafloor massive sulphide mining. Ore Geol. Rev. 86, 309–337. http://dx.doi.org/10.1016/j.oregeorev.2017.02.028.

Feely, R.A., Lewison, M., Massoth, G.J., Robert-Baldo, G., Lavelle, J.W., Byrne, R.H., Von Damm, K.L., Curl, H.C., 1987. Composition and dissolution of black smoker particulates from active vents on the Juan de Fuca Ridge. J. Geophys. Res. 92, 11347–11363. http://dx.doi.org/10.1029/JB092iB11p11347.

Franklin, N.M., Stauber, J.L., Lim, R.P., 2001. Development of flow cytometry-based algal bioassays for assessing toxicity of copper in natural waters. Environ. Toxicol. Chem. 20, 160–170. http://dx.doi.org/10.1002/etc.5620200118.

Fullston, D., Fornasiero, D., Ralston, J., 1999. Zeta potential study of the oxidation of copper sulfide minerals. Colloids Surf. A Physicochem. Eng. Asp. 146, 113–121. http://dx.doi.org/10.1016/S0927-7757(98)00725-0.

German, C.R., Petersen, S., Hannington, M.D., 2016. Hydrothermal exploration of mid-ocean ridges: where might the largest sulfide deposits be forming? Chem. Geol. 420, 114–126. http://dx.doi.org/10.1016/j.chemgeo.2015.11.006.

Gilbert, T., King, B., Benfer, N., Terrens, G., 2008. Appendix 12: Modelling the Dispersion of the Returned Water Discharge Plume From the Solwara 1 Seabed Mining Project, Manus Basin, Papua New Guinea.

Gwyther, D., 2008. Environmental IMPACT statement, Solwara 1 project. In: Main Report Coffey Natural Systems, (Brisbane).

Hannington, M.D., 1993. The formation of atacamite during weathering of sulfides on the modern seafloor. Can. Mineral. 31, 945–956.

Hannington, M., Jamieson, J., 2011. Estimating the metal content of SMS deposits. In: Oceans. IEEE.

Hannington, M., Herzig, P., Scott, S., Thompson, G., Rona, P.A., 1991. Comparative mineralogy and geochemistry of gold-bearing sulfide deposits on the mid-ocean ridges. Mar. Geol. 101, 217–248. http://dx.doi.org/10.1016/0025-3227(91)90073-D.

Hannington, M.D., de Ronde, C.E.J., Petersen, S., 2005. Modern seafloor tectonics and submarine hydrothermal systems. In: Economic Geology: One Hundredth Anniversary Volume: 1905–2005. Society of Economic Geologists. http://dx.doi.org/10.1029/GM091p0115.

Hannington, M.D., Jamieson, J., Monecke, T., Petersen, S., 2010. Modern sea-floor massive sulfides and base metal resources: toward an estimate of global sea-floor massive sulfide potential. Soc. Econ. Geol. Spec. Publ. 15 (15), 317–338.

Heidel, C., Tichomirowa, M., Junghans, M., 2013. Oxygen and sulfur isotope investigations of the oxidation of sulfide mixtures containing pyrite, galena, and sphalerite. Chem. Geol. 342, 29–43. http://dx.doi.org/10.1016/j.chemgeo.2013.01.016.

Herzig, P.M., Hannington, M.D., 1995. Polymetallic massive sulfides at the modern seafloor a review. Ore Geol. Rev. 10, 95–115. http://dx.doi.org/10.1016/0169-1368(95)00009-7.

Humphris, S.E., Herzig, P.M., Miller, D.J., Alt, J.C., Becker, K., Brown, D., Brügmann, G., Chiba, H., Fouquet, Y., Gemmell, J.B., Guerin, G., Hannington, M.D., Holm, N.G., Honnorez, J.J., Iturrino, G.J., Knott, R., Ludwig, R., Nakamura, K., Petersen, S., Reysenbach, A.-L., Rona, P.A., Smith, S., Sturz, A.A., Tivey, M.K., Zhao, X., 1995. The internal structure of an active sea-floor massive sulphide deposit. Nature 377, 713–716. http://dx.doi.org/10.1038/377713a0.

Humphris, S.E., Herzig, P.M., Miller, D.J., 1996. 158: College Station, TX (Ocean Drilling Program). Proc. ODP, Init. Repts.

International Seabed Authority (ISA), 2017. Deep seabed minerals contractors. Available at: https://www.isa.org.jm/deep-seabed-minerals-contractors.

John, M., Heuss-Aßbichler, S., Ullrich, A., 2016. Conditions and mechanisms for the formation of nano-sized Delafossite ($CuFeO_2$) at temperatures ≤ 90 °C in aqueous solution. J. Solid State Chem. 234, 55–62. http://dx.doi.org/10.1016/j.jssc.2015.11.033.

Jong, T., Parry, D.L., 2004. Adsorption of Pb(II), Cu(II), Cd(II), Zn(II), Ni(II), Fe(II), and As(V) on bacterially produced metal sulfides. J. Colloid Interface Sci. 275, 61–71. http://dx.doi.org/10.1016/j.jcis.2004.01.046.

Jyothi, N., Sudha, K.N., Natarajan, K.A., 1989. Electrochemical aspects of selective bioleaching of sphalerite and chalcopyrite from mixed sulphides. Int. J. Miner. Process. 27, 189–203. http://dx.doi.org/10.1016/0301-7516(89)90064-1.

Koleini, S.M.J., Jafarian, M., Abdollahy, M., Aghazadeh, V., 2010. Galvanic leaching of chalcopyrite in atmospheric pressure and sulfate media: kinetic and surface studies. Ind. Eng. Chem. Res. 49, 5997–6002. http://dx.doi.org/10.1021/ie100017u.

Kolta, G.A., El-Tawil, S.Z., Ibrahim, A.A., Felix, N.S., 1981. Kinetics and mechanism of copper ferrite formation. Thermochim. Acta 43, 279–287. http://dx.doi.org/10.1016/0040-6031(81)85185-4.

Koski, R.A., 2012. Supergene ore and gangue characteristics in volcanogenic massive sulfide occurrence model. In: U.S. Geological Survey Scientific Investigations Report 2010 5070 C, (chap. 12).

Koski, R.A., Munk, L., Foster, A.L., Shanks, W.C., Stillings, L.L., 2008. Sulfide oxidation and distribution of metals near abandoned copper mines in coastal environments, Prince William Sound, Alaska, USA. Appl. Geochem. 23, 227–254. http://dx.doi.org/10.1016/j.apgeochem.2007.10.007.

Kwong, Y.T.J., Swerhone, G.W., Lawrence, J.R., 2003. Galvanic sulphide oxidation as a metal-leaching mechanism and its environmental implications. Geochem.: Explor., Environ., Anal. 3, 337–343. http://dx.doi.org/10.1144/1467-7873/03/013.

Le Roux, S.G., Miller, J.A., Dunford, A.J., Clarke, C.E., 2016. The dissolution kinetics of atacamite in the acid range and the stability of atacamite containing soils from Namaqualand, South Africa. Appl. Geochem. 64, 22–29. http://dx.doi.org/10.1016/j.apgeochem.2015.09.003.

Li, Z., Heping, L., Liping, X., 2006. Galvanic interaction between galena and pyrite in an open system. Chin. J. Geochem. 25, 230–237. http://dx.doi.org/10.1007/BF02840416.

Liu, C., Huang, P.M., 2003. Kinetics of lead adsorption by iron oxides formed under the influence of citrate. Geochim. Cosmochim. Acta 67, 1045–1054. http://dx.doi.org/10.1016/S0016-7037(02)01036-0.

Liu, X., Millero, F.J., 2002. The solubility of iron in seawater. Mar. Chem. 77, 43–54. http://dx.doi.org/10.1016/S0304-4203(01)00074-3.

Liu, Q., Li, H., Zhou, L., 2008. Galvanic interactions between metal sulfide minerals in a flowing system: implications for mines environmental restoration. Appl. Geochem. 23, 2316–2323. http://dx.doi.org/10.1016/j.apgeochem.2008.02.024.
Lizama, H.M., Suzuki, I., 1991. Interaction of chalcopyrite and sphalerite with pyrite during leaching by *Thiobacillus ferrooxidans* and *Thiobacillus thiooxidans*. Can. J. Microbiol. 37, 304–311. http://dx.doi.org/10.1139/m91-047.
Majima, H., 1969. How oxidation affects selective flotation of complex sulphide ores. Can. Metall. Q. 8, 269–273.
Majuste, D., Ciminelli, V.S.T., Osseo-Asare, K., Dantas, M.S.S., 2012. Quantitative assessment of the effect of pyrite inclusions on chalcopyrite electrochemistry under oxidizing conditions. Hydrometallurgy 113–114, 167–176. http://dx.doi.org/10.1016/j.hydromet.2011.12.020.
Malmström, M., Collin, C., 2004. Sphalerite weathering kinetics: effect of pH and particle size. In: Proc. 11th Symp. Water-Rock Interact. vol. 1. pp. 849–852.
Mann, A.W., Deutscher, R.L., 1980. Solution geochemistry of lead and zinc in water containing carbonate, sulphate and chloride ions. Chem. Geol. 29, 293–311. http://dx.doi.org/10.1016/0009-2541(80)90026-1.
McBeth, J.M., Little, B.J., Ray, R.I., Farrar, K.M., Emerson, D., 2011. Neutrophilic iron-oxidizing "Zetaproteobacteria" and mild steel corrosion in nearshore marine environments. Appl. Environ. Microbiol. 77, 1405–1412. http://dx.doi.org/10.1128/AEM.02095-10.
McKibben, M.A., Barnes, H.L., 1986. Oxidation of pyrite in low temperature acidic solutions: rate laws and surface textures. Geochim. Cosmochim. Acta 50, 1509–1520. http://dx.doi.org/10.1016/0016-7037(86)90325-X.
Mehta, A.P., Murr, L.E., 1982. Kinetic study of sulfide leaching by galvanic interaction between chalcopyrite, pyrite, and sphalerite in the presence of *T. ferrooxidans* (30 °C) and a thermophilic microorganism (55 °C). Biotechnol. Bioeng. 24, 919–940. http://dx.doi.org/10.1002/bit.260240413.
Mehta, A.P., Murr, L.E., 1983. Fundamental studies of the contribution of galvanic interaction to acid-bacterial leaching of mixed metal sulfides. Hydrometallurgy 9, 235–256. http://dx.doi.org/10.1016/0304-386X(83)90025-7.
Millero, F.J., 2013. Chemical Oceanography, fourth edition. CRC Press.
Mills, R.A., Elderfield, H., 1995. Rare earth element geochemistry of hydrothermal deposits from the active TAG Mound, 26°N Mid-Atlantic Ridge. Geochim. Cosmochim. Acta 59, 3511–3524.
Monecke, T., Petersen, S., Hannington, M.D., Grant, H., Samson, I., 2016. The minor element endowment of modern sea-floor massive sulfide deposits and comparison with deposits hosted in ancient volcanic successions. Rev. Econ. Geol. 18, 245–306.
Moses, C.O., Herman, J.S., 1991. Pyrite oxidation at circumneutral pH. Geochim. Cosmochim. Acta 55, 471–482. http://dx.doi.org/10.1016/0016-7037(91)90005-P.
Moses, C.O., Kirk Nordstrom, D., Herman, J.S., Mills, A.L., 1987. Aqueous pyrite oxidation by dissolved oxygen and by ferric iron. Geochim. Cosmochim. Acta 51, 1561–1571. http://dx.doi.org/10.1016/0016-7037(87)90337-1.
Murr, L.E., 2006. Biological issues in materials science and engineering: interdisciplinarity and the bio-materials paradigm. JOM 58, 23–33. http://dx.doi.org/10.1007/s11837-006-0136-3.
Natarajan, K.A., 1985. Microbe-mineral interactions of relevance in the hydrometallurgy of complex sulphides. In: Mehrotra, S.P., Ramachandran, T.R. (Eds.), Progress in Metallurgical Research-Fundamental and Applied Aspects. Tata McGraw Hill, New Delhi, New Delhi, pp. 105–112.
Natarajan, K., 1988. Electrochemical aspects of bioleaching multisulfide minerals. Miner. Metall. Process. 5, 61–65.
Natarajan, K.A., Iwasaki, I., 1983. Role of galvanic interactions in the bioleaching of Duluth gabbro copper-nickel sulfides. Sep. Sci. Technol. 18, 1095–1111. http://dx.doi.org/10.1080/01496398308059919.
Natarajan, K., Iwasaki, I., 1986. Microbe-mineral interactions in the leaching of complex sulfides. In: Clum, J.A., Haas, L.A. (Eds.), Microbiological Effects on Metallurgical Processes. TMS AIME, New York, New York.
Parry, D.L., 2008. Solwara 1 Project Elutriate Report Phase 1 and 2.
Patwardhan, A.M., 2012. The dynamic earth system, third ed. PHI Learning, New Delhi.
Plumlee, G., Logsdon, M., Filipek, L., 1999. The environmental geology of mineral deposits. In: The Environmental Geochemistry of Mineral Deposits. Society of Economic Geologists, pp. 71–116.
Pollard, A.M., Thomas, R.G., Williams, P.A., 1989. Synthesis and Stabilities of the Basic Copper(II) Chlorides Atacamite, Paratacamite and Botallackite. vol. 53. pp. 557–563.
Ridley, W.I., 2012. Weathering processes, volcanogenic massive sulfide occurrence model. In: U.S. Geological Survey Scientific Investigations Report 2010-5070-C.
Rimstidt, J.D., Newcomb, W.D., 1993. Measurement and analysis of rate data: the rate of reaction of ferric iron with pyrite. Geochim. Cosmochim. Acta 57, 1919–1934. http://dx.doi.org/10.1016/0016-7037(93)90084-A.
Rimstidt, J.D., Chermak, J.A., Gagen, P.M., 1994. Rates of reaction of galena, sphalerite, chalcopyrite, and arsenopyrite with Fe (III) in acidic solutions. In: Alpers, C.N., Blowes, D.W. (Eds.), Environmental Geochemistry of Sulfide Oxidation. American Chemical Society, Washington, DC, pp. 2–13. http://dx.doi.org/10.1021/bk-1994-0550.ch001.
Romano, G.Y., 2012. Kinetics of Pyrrhotite Oxidation in Seawater: Implications for Mining Seafloor Hotsprings.
Rose, A.W., Bianchi-Mosquera, G.C., 1993. Adsorption of Cu, Pb, Zn, Co, Ni, and Ag on goethite and hematite; a control on metal mobilization from red beds into stratiform copper deposits. Econ. Geol. 88, 1226–1236. http://dx.doi.org/10.2113/gsecongeo.88.5.1226.
Salmon, S.U., Malmström, M.E., 2006. Quantification of mineral dissolution rates and applicability of rate laws: laboratory studies of mill tailings. Appl. Geochem. 21, 269–288. http://dx.doi.org/10.1016/j.apgeochem.2005.09.014.
Sander, S.G., Koschinsky, A., 2011. Metal flux from hydrothermal vents increased by organic complexation. Nat. Geosci. 4, 145–150.
Savenko, V., Shatalov, I., 1998. Atacamite Solubilities and the Physicochemical State of Solute Copper in Seawater. Geochem. Int. 36, 752–756.
Schlitzer, R., 2000. Electronic atlas of WOCE hydrographic and tracer data now available. Eos. Trans. AGU 81.
Seal, R.R.I., Foley, N.K., 2002. Progress on geoenvironmental models for selected mineral deposit types. In: Publ. US Geol. Surv, pp. 83.
Simpson, S., Angel, B., Hamilton, I., Spadaro, D., Binet, M., 2007. Water and Sediment Characterisation and Toxicity Assessment for the Solwara 1 Project.
Subrahmanyam, T.V., Forssberg, K.S.E., 1993. Mineral solution-interface chemistry in minerals engineering. Miner. Eng. 6, 439–454. http://dx.doi.org/10.1016/0892-6875(93)90173-K.
Swallow, K.C., Morel, F., 1980. Adsorption of trace metals by hydrous ferric oxide in seawater. Rhode Island.
Taylor, R., 2011. Gossans and Leached Cappings: Field Assessment. Springer Science & Business Media.
Webber, A.P., Roberts, S., Murton, B.J., Hodgkinson, M.R.S., 2015. Geology, sulfide geochemistry and supercritical venting at the Beebe Hydrothermal Vent Field, Cayman Trough. Geochem. Geophys. Geosyst. 16, 2661–2678. http://dx.doi.org/10.1002/2015GC005879.
Weisener, C.G., Smart, R.S.C., Gerson, A.R., 2004. A comparison of the kinetics and mechanism of acid leaching of sphalerite containing low and high concentrations of iron. Int. J. Miner. Process. 74, 239–249. http://dx.doi.org/10.1016/j.minpro.2003.12.001.
Wohlgemuth-Ueberwasser, C.C., Viljoen, F., Petersen, S., Vorster, C., 2015. Distribution and solubility limits of trace elements in hydrothermal black smoker sulfides: an in-situ LA-ICP-MS study. Geochim. Cosmochim. Acta 159, 16–41. http://dx.doi.org/10.1016/j.gca.2015.03.020.
Yelloji Rao, M.K., Natarajan, K.A., 1989. Electrochemical effects of mineral-mineral interactions on the flotation of chalcopyrite and sphalerite. Int. J. Miner. Process. 27, 279–293. http://dx.doi.org/10.1016/0301-7516(89)90069-0.